Available online at www.sciencedirect.com
SCIENCE DIRECT®
ELSEVIER
PEPTIDES
Peptides 25 (2004) 433–464
www.elsevier.com/locate/peptides

Review

Galanin in the brain: chemoarchitectonics and brain cartography—a historical review☆

David M. Jacobowitz[a,b,*], Adelheid Kresse[c], Gerhard Skofitsch[c]

[a] Laboratory of Clinical Science, National Institutes of Health, NIMH, Bethesda, MD 20892, USA
[b] Department of Anatomy, Physiology and Genetics, Uniformed Services University, Building C, Room C2099, 4301 Jones Bridge Road, Bethesda, MD 20814, USA
[c] Section of Wildlife Research and Parasitology, Department of Zoology, University of Graz, A-1080 Graz, Austria

Abstract

We present a review of galanin in the brain from a historical perspective of the development of "chemoarchitectonics" and "brain cartography" accomplished in the Histopharmacology Section at the National Institutes of Health. It was the mapping of potential brain neuroregulators that served as a springboard of ideas from which behavioral studies emanate. The integration of the known localization of neurotransmitter/neuromodulatory nerves ("chemoarchitectonic maps") and receptor binding sites with biochemical data derived from brain micropunches coupled with behavioral analysis at the level of discrete brain allows one to define the anatomical circuits which support behavioral changes and which ultimately will improve our understanding of mental disorders.

Keywords: Galanin; Brain; Histochemistry; Brain cartography; Chemoarchitectonics; Brain maps; Neuropeptides; In situ hybridization histochemistry; Brain atlas; Colocalization; Gene expression

1. Introduction and historical perspective

I am very pleased that the immunohistochemical mapping of galanin-containing neurons in the rat CNS [88] in my laboratory was one of the most cited papers ever published in *Peptides*. This paper was part of a series of publications in *Peptides* that was also highly cited [70,83,84,87,92]. At NIMH, my section on Histopharmacology is a unique laboratory dedicated to the belief that the challenge of uncovering the secrets to brain function lies in the unraveling of neuronal connectivity. To this end, a portion of our work has been involved in mapping of neuronal systems of the brain. The guiding principle is that knowledge of the building blocks gives us clues about both how the nervous systems operate and how they might fail due to disease and injury. Our laboratory has produced complete maps of 12 whole brain neuronal systems—more than have come out of any other laboratory in the world: catecholamines/serotonin [33,36,73]; α-melanocyte stimulating hormone [34]; bovine pancreatic polypeptide [68]; motilin [35]; gonadotropin releasing factor [38]; atrial naturetic factor [39]; corticotropin releasing factor [85]; galanin [88]; calcitonin gene-related peptide [83]; melanin concentrating hormone-like peptide [91]; atrial natriuretic factor [89] in addition to an atlas of the chemoarchitectonics of the developing mouse brain [31]. The major "depository" of information concerning sites of localization for potent brain neurochemicals has given birth to a field of neuroscience that I have described as "Brain Cartography".

In the 1970s, our Section was involved with studies concerning major neurotransmitters and their associated receptor binding sites. In addition to histochemical and immunocytochemical studies concerning the mapping of the localization of brain neuronal systems, another major program was underway regarding the biochemical mapping of the discrete localization of neurochemicals within the brain. The "micropunch" technique [30,72] is a unique method whereby discrete nuclei are "punched" out of fresh and frozen brain slices and collected in appropriate diluents. A variety of neurochemicals were assayed by several methods such as the radiomicroenzymatic procedures for neurotransmitters/enzymes and radioimmunoassays for peptides that were available at that time.

These neurochemical maps were very useful adjuncts to the histochemical maps that were already published.

☆ DOI of original article: 10.1016/0196-9781(85)90118-4.
* Corresponding author. Tel.: +1-301-295-3519; fax: +1-301-295-3566.
E-mail address: dwj@helix.nih.gov (D.M. Jacobowitz).

0196-9781/$ – see front matter © 2004 Elsevier Inc. All rights reserved.
doi:10.1016/j.peptides.2004.02.015

Important findings evolved from this technology using stereotaxic lesions in the brain to determine sites of localization of major neuronal pathways emanating from a single source such as the locus coeruleus for noradrenergic pathways and the arcuate nucleus for α-MSH (proopiomelanocortin, POMC) pathways. We were also able to study the influence of a variety of behaviors, stressors and genetic mutants on specific neurochemicals. Thus, it was the mapping of potential brain neuroregulators that served as a springboard of ideas from which behavioral studies emanate. For example, knowledge of the localization of peptides in the brain enabled us to use a discrete microinjection technique to examine the effects on blood pressure and heart rate following injections of a variety of neuropeptides (α-MSH, TRH, bradykinin, dermorphin, CGRP, ANF) into discrete nuclei of the hypothalamus and preoptic area (see [12–16,66,80]). The data demonstrated the diversity of central cardiovascular actions of these peptides and emphasized the advantage of microinjection methods in defining central cardiovascular effects. Unlike either intracerebroventricular injections or electrical stimulations, the results of which represent a more widespread involvement of neuronal structures, intraparenchymal injections allowed us to localize the discrete anatomical sites for cardiovascular actions and to provide preliminary information on the peripheral mechanism(s) responsible for the effects elicited at each site by each peptide.

In summary, the integration of the known localization of neurotransmitter/neuromodulatory nerves ("maps") and receptor binding sites with biochemical data derived from brain micropunches coupled with behavioral analysis at the level of discrete brain nuclei allows one to define the anatomical circuits which support behavioral changes and which ultimately will improve our understanding of mental disorders.

2. Stereotaxic atlas of galanin distribution

Rational approaches to the study of the function of central galanin require the knowledge of the distinct localization of the peptide and the receptors in the central nervous system. In this work we review detailed stereotaxic maps of the distribution of galanin-ir neurons and receptor binding sites in the rat brain using indirect immunofluorescence methods and in vitro autoradiographic techniques. A comparison of the localization of peptide, receptor binding sites is presented, as well as quantitative values of galanin-ir in discrete regions of the rat brain and the distribution of galanin mRNA-labeled cells and studies on the characterization of the molecular heterogeneity of galanin-ir in certain areas. We also review the colocalization of galanin-ir with classical neurotransmitters, amines and other neuropeptides in brain and related structures, the central actions of galanin on the control of biogenic amines and the release of a variety of neurochemicals.

Immunohistochemical mapping of galanin-like neurons in the rat central nervous system

Gerhard Skofitsch, David M. Jacobowitz

Peptides 1985;6:509–46

Abstract

Using an antiserum generated in rabbits against synthetic galanin (GA) and the indirect immunofluorescence method, the distribution of GA-like immunoreactive cell bodies and nerve fibers was studied in the rat central nervous sytem (CNS) and a detailed stereotaxic atlas of GA-like neurons was prepared. GA-like immunoreactivity was widely distributed in the rat CNS. Appreciable numbers of GA-positive cell bodies were observed in the rostral cingulate and medial prefrontal cortex, the nucleus interstitialis striae terminalis, the caudate, medial preoptic, preoptic periventricular, and preoptic suprachiasmatic nuclei, the medial forebrain bundle, the supraoptic, the hypothalamic periventricular, the paraventricular, the arcuate, dorsomedial, perifornical, thalamic periventricular, anterior dorsal and lateral thalamic nuclei, medial and central amygdaloid nuclei, dorsal and ventral premamillary nuclei, at the base of the hypothalamus, in the central gray matter, the hippocampus, the dorsal and caudoventral raphe nuclei, the interpeduncular nucleus, the locus coeruleus, ventral parabrachial, solitarii and commissuralis nuclei, in the Al, Cl and A4 catechaolamine areas, the posterior area postrema and the trigeminal and dorsal root ganglia. Fibers were generally seen where cell bodies were observed. Very dense fiber bundles were noted in the septohypothalamic tract, the preoptic area, in the hypothalamus, the habenula and the thalamic periventricular nucleus, in the ventral hippocampus, parts of the reticular formation, in the locus coeruleus, the dorsal parabrachial area, the nucleus and tract of the spinal trigeminal area and the substantia gelatinosa, the superficial layers of the spinal cord and the posterior lobe of the pituitary. The localization of the GA-like immunoreactivity in the locus coeruleus suggests a partial coexistence with catecholaminergic neurons as well as a possible involvement of the GA-like peptide in a neuroregulatory role.

Keywords: Galanin; Rat; Brain; Central nervous system; Sensory ganglia; Immunohistochemistry

In situ hybridization histochemistry (ISHH) complements the ability of standard immunocytochemical procedures to detect cellular peptides and proteins, because the combined use of these techniques provides a cross-check of their specificity. Similar patterns of cellular staining found when using both of these techniques provide confirmation of hybridization probe and antiserum specificity. ISHH may also extend immunocytochemistry results by addressing the issue of whether a positively stained cell has synthesized the detected peptide or acquired it by means of uptake from the extracellular space. A complete mapping of the distribution of galanin mRNA-labeled cells was prepared and compared with maps of immunoreactive cell bodies of colchicine-treated rats.

A complete stereotaxic atlas showing the discrete distribution of galanin-immunoreactive (ir) nerves and cell bodies, mRNA-labeled cells and receptor binding sites [7,88,92] was prepared according to the maps of Jacobowitz and Palkovits and Palkovits and Jacobowitz [36,73], using indirect immunofluorescence techniques [8] with modifications to standard immunocytochemical procedures described in detail previously [83,86,88,89]. Stereotaxic coordinates were defined according to the atlases of König and Klippel [44] and Paxinos and Watson [75].

Untreated rats and rats pretreated with colchicine (i.c.v.) 2 days prior to the experiment were perfused via the heart with 10% formalin. The brain and spinal cord were removed and frozen on dry ice. Coronal cryostat sections (20 μm) were processed for indirect immunocytochemistry. The sections were incubated in the galanin antiserum diluted 1:1000 to 1:2000 for 3 days followed by an incubation in FITC conjugated goat anti-rabbit IgG diluted 1:400 for 30 min. Fluorescence was monitored using a Leitz Orthoplan fluorescence microscope equipped with a dark-field condenser and a Ploempak illuminator. The antiserum used was raised in rabbits against synthetic porcine galanin coupled to human thyroglobulin by the carbodiimide reaction [20] and was obtained commercially (Peninsula Labs, Belmont, CA). The following substances did not cross-react in galanin-radioimmunoassay (RIA) up to 10 ng per tube: substance P; vasopressin; neurokinin A; the neuromedins B, C and K; kassinin; eledoisin; physalaemin; bombesin; rat-calcitonin-gene related peptide; and vasoactive intestinal polypeptide. The last four carboxy-terminal amino acids of galanin are structurally similar to physalaemin and substance P. Otherwise the amino acid sequence of galanin did not correspond to that of any other known peptide [97]. As an immunohistochemical control, the antiserum was preadsorbed with 1 μM synthetic galanin, which resulted in a complete loss of immunostaining in all areas investigated. Preadsorption of the antiserum with 10 μM synthetic substance P, somatostatin, cholecystokinin 8, vasoactive intestinal polypeptide, vasopressin, corticotropin releasing factor and rat calcitonin-gene-related peptide did not visibly affect the immunostaining.

The galanin antiserum revealed a discrete localization of cell bodies and fibers throughout the rat central nervous system. Galanin-ir cell bodies were observed in colchicine pretreated rats only; nerve fibers were observed in colchicine pretreated, untreated rats and autoradiographic distribution of ^{125}I-galanin binding sites. A complete stereotaxic mapping of galanin-ir cell bodies and fibers is presented in Figs. 1–9. Galanin binding sites were found to be distributed in discrete areas of the rat brain. Autoradiographic images and corresponding schematic drawings of anterior olfactory regions of the rat brain showing galanin receptors are shown in Fig. 10. Fig. 11 shows darkfield photomicrographs of galanin mRNA-containing neurons in the arcuate nucleus/median eminence, supraoptic nucleus, subfornical organ and cerebellum Purkinje cells (see [88] for additional photographs).

3. Receptor autoradiography

Using autoradiographic techniques and [^{125}I]-galanin (New England Nuclear, Boston, MA; specific activity 2200 Ci/mmol) receptor binding sites have been demonstrated in coronal sections throughout the rat brain [92]. From the very beginning of receptor autoradiography it has become apparent that neuropeptide receptor binding sites are not always located in close proximity to neurotransmitter containing neuronal fibers or terminal fields [22]. Such ‘mismatches’ are the subject of considerable speculation. Nevertheless autoradiography and topographical localization of neuropeptide binding sites are important dimensions which allow us to demonstrate potential sites of release and action of neuropeptides in the brain.

Very dense binding sites were observed in the central, medial, basal and cortical nuclei of the amygdala. *Dense galanin binding* appeared to build a continuity between the prefrontal cortex and the anterior nucleus of the olfactory bulb. Dense binding sites were also noted in the dorsal septal nucleus, the dorsal bed nucleus of the stria terminalis close to the internal capsule the ventral pallidum, the internal medullary lamina of the thalamus and the medial pretectal nucleus. In the hindbrain dense galanin binding sites were found in the borderline area of the spinal trigeminal nucleus towards the spinal trigeminal tract with a continuity to the substantia gelatinosa and the superficial layers (layers I and II) of the spinal cord.

A comparison of the distribution of the galanin binding sites with the localization of galanin-ir fibers reveals a good correlation of high-density immunoreactive fibers and binding sites in most of the thalamic and hypothalamic nuclei and the sensory terminal areas of the medulla oblongata and the spinal cord. Mismatches between nerves and binding sites (i.e., dense binding sites and sparse numbers of nerves) were observed in the olfactory tubercle, the piriform cortex, the superior colliculus, the nucleus of the lateral olfactory tract and the nucleus accumbens. The significance of mismatches between neuronal varicosities and receptor binding sites is a matter of speculation [22]. The absence of histochemically demonstrable terminal fibers may be a reflection of neuronal populations in certain discrete areas which lack peptide binding sites within terminal fields.

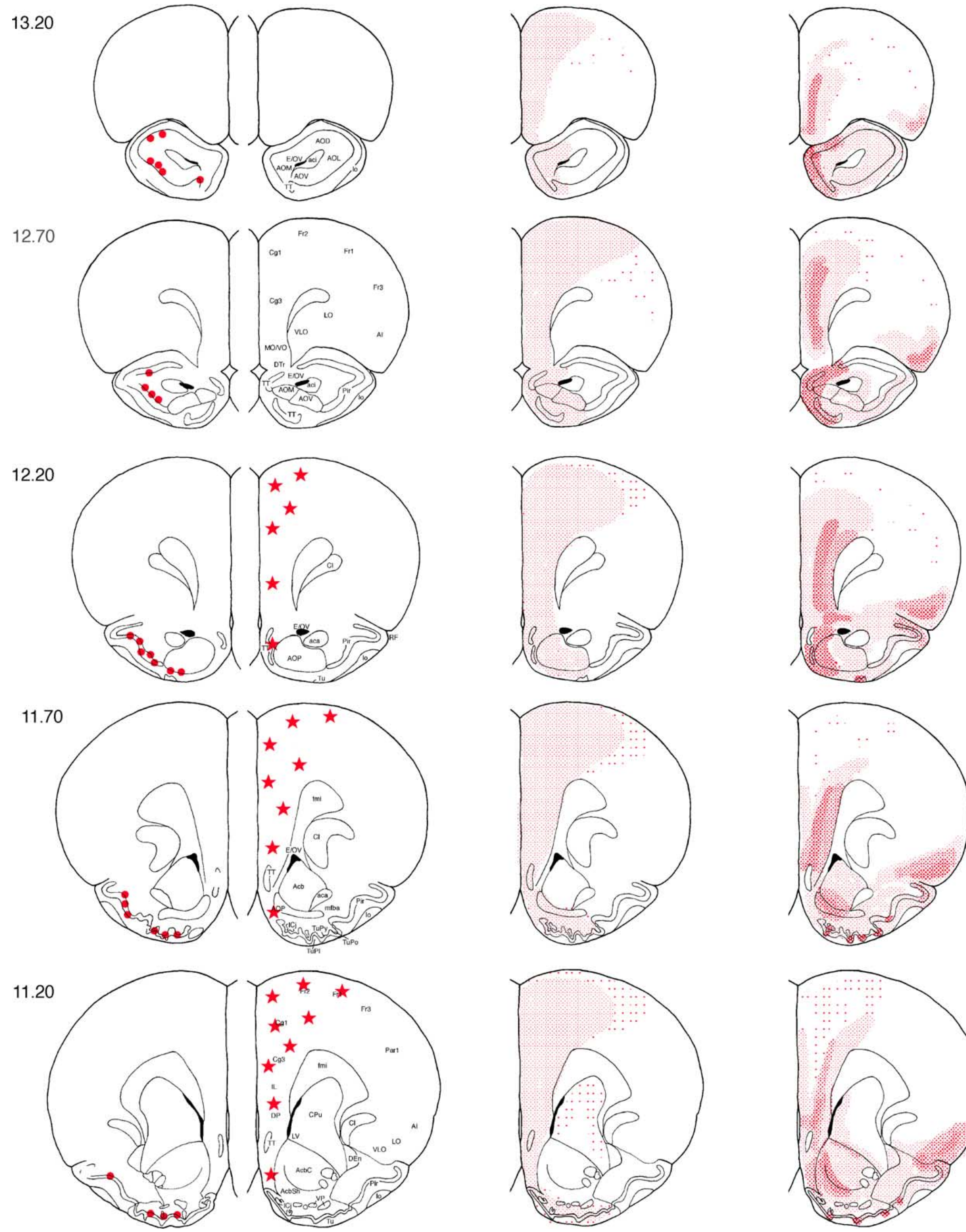

Figs. 1–9. Schematical drawings representing a complete stereotaxic mapping of galanin mRNA containing neurons (dots, far left), galanin immunoreactive neuronal cell bodies (left, asterisks), immunoreactive nerves and fibers (right, shadings) and galanin receptors (far right, shadings) in the rat central nervous system. Terminology and modified planes are based on the atlases of Paxinos and Watson (1982, 1986), arranged from rostral to caudal. Coordinates are given in mm anterior or posterior to the interaural plane (level 0.00). The symbols do not represent quantitative distribution of labeled neurons.

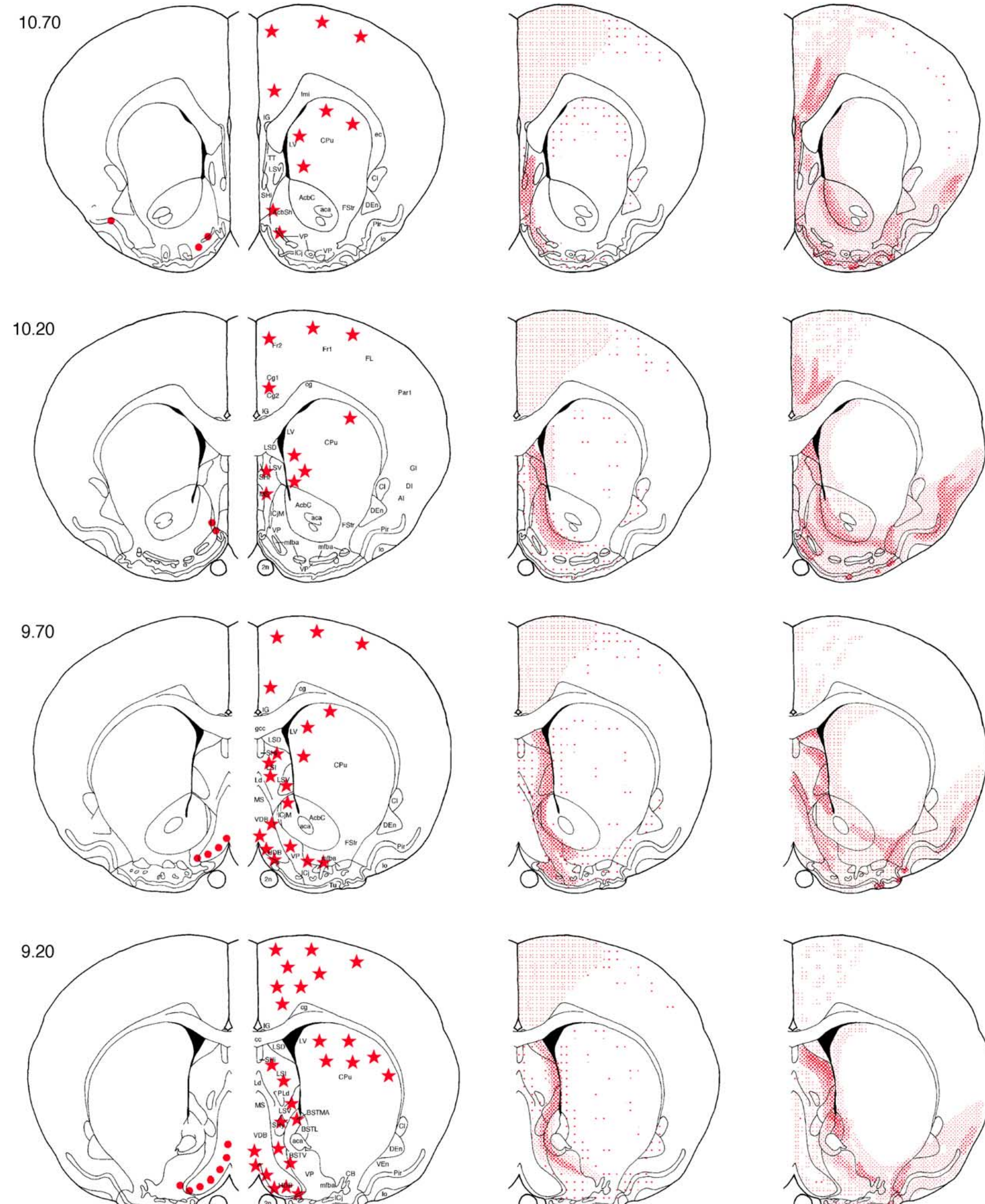

Figs. 1–9. (*Continued*)

These areas may reflect a high turnover of the peptide. Fixation perfusion with formalin could easily result in diffusion of the small amount of peptide present. The presence of radioimmunoassayable galanin in areas such as the superior colliculus and the nucleus accumbens suggests the presence of the peptide, which may have been depleted following fixation perfusion. Such a poor peptide binding capacity, coupled to a site of dense receptor binding, can be offered as

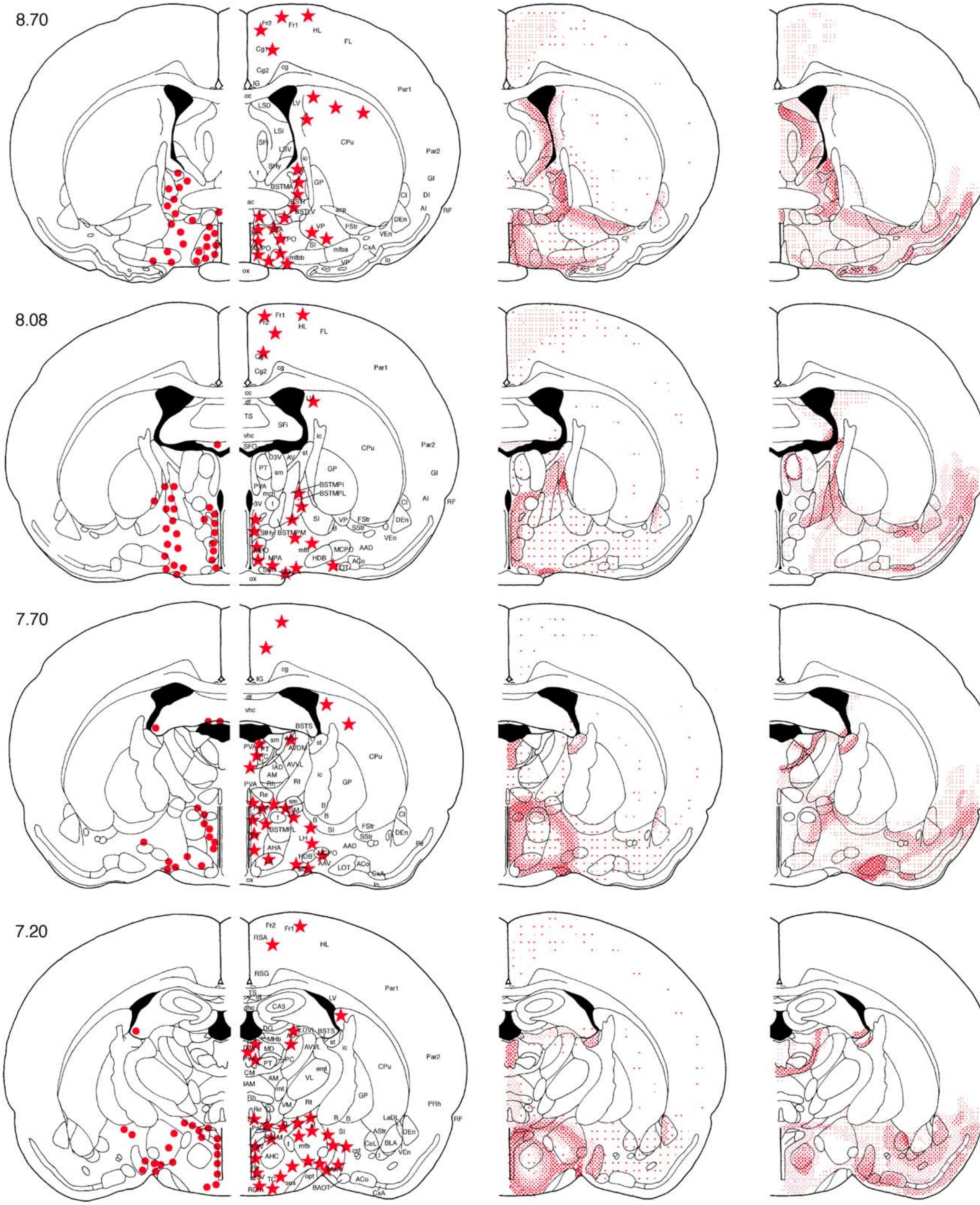

Figs. 1–9. (*Continued*)

an explanation for mismatches observed with other neurochemicals.

The high density of binding sites in the nucleus of the lateral olfactory tract and the piriform cortex may be a reflection of a very active modulation of olfactory function by galanin. It is interesting that the rhinencephalon, i.e., those structures of the central nervous system that receive fibers from the olfactory bulb (e.g., the anterior olfactory nucleus,

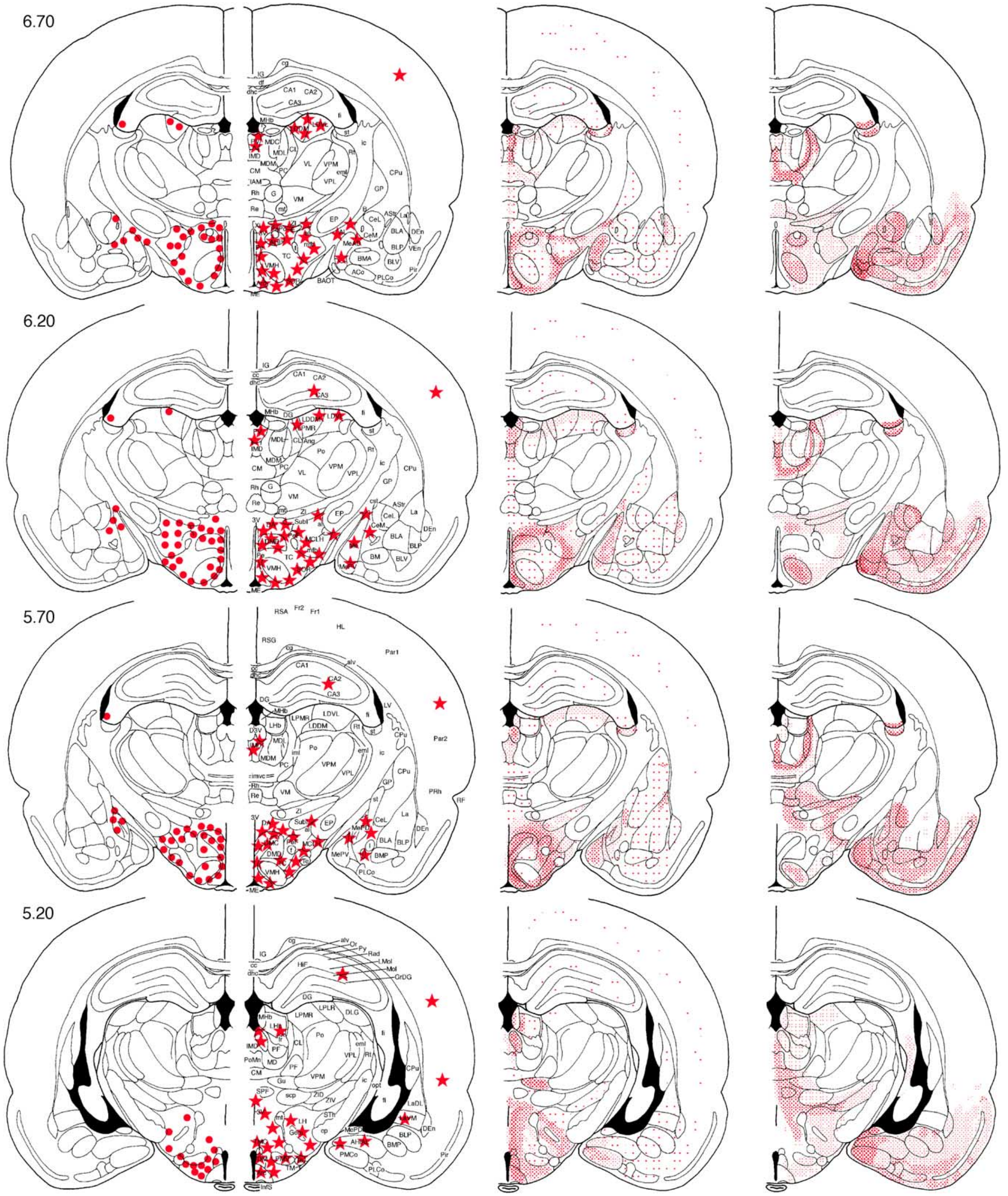

Figs. 1–9. (*Continued*)

the olfactory tubercle, parts of the amygdaloid complex and the piriform cortex), was outstanding in terms of receptor binding sites. Furthermore, the piriform lobe, which contains the entorhinal cortex in addition to the prepiriform and the periamygdaloid cortices, also contains abundant receptor binding sites. This further focuses attention on the possible involvement of galanin in olfactory sensation. The autoradiographic data suggest a ‘functional connectivity’ between

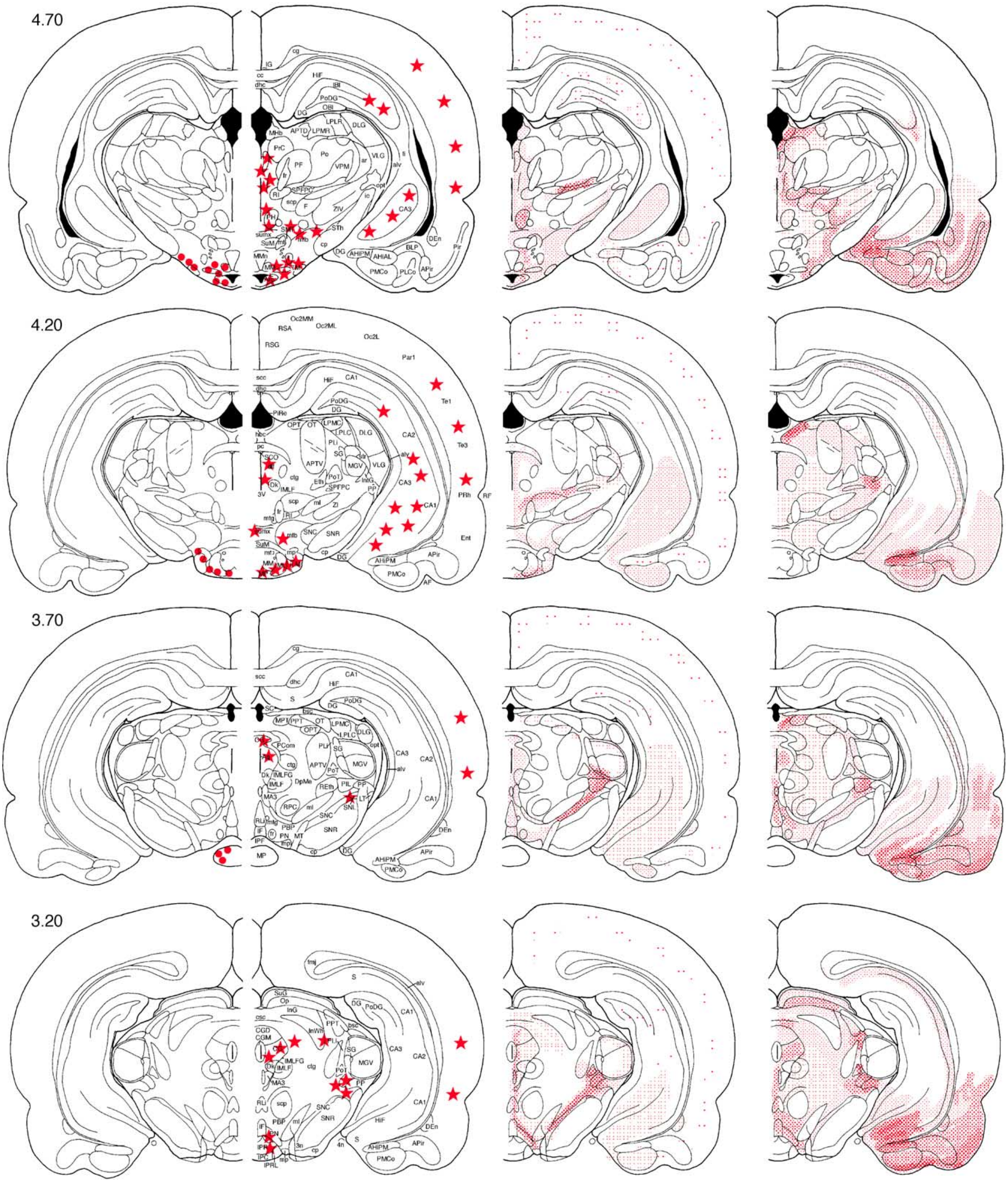

Figs. 1–9. (*Continued*)

the anterior olfactory nucleus and the prefrontal cortex. This suggests a site where the limbic system may directly receive olfactory impulses. Such a receptor 'connectivity' between the olfactory system and the limbic system suggests modulatory influences between these systems. This could allow the animal to cope with environmental olfactory cues.

It is also interesting that most of the efferent projections of the amygdaloid complex as reported in the rat, cat or

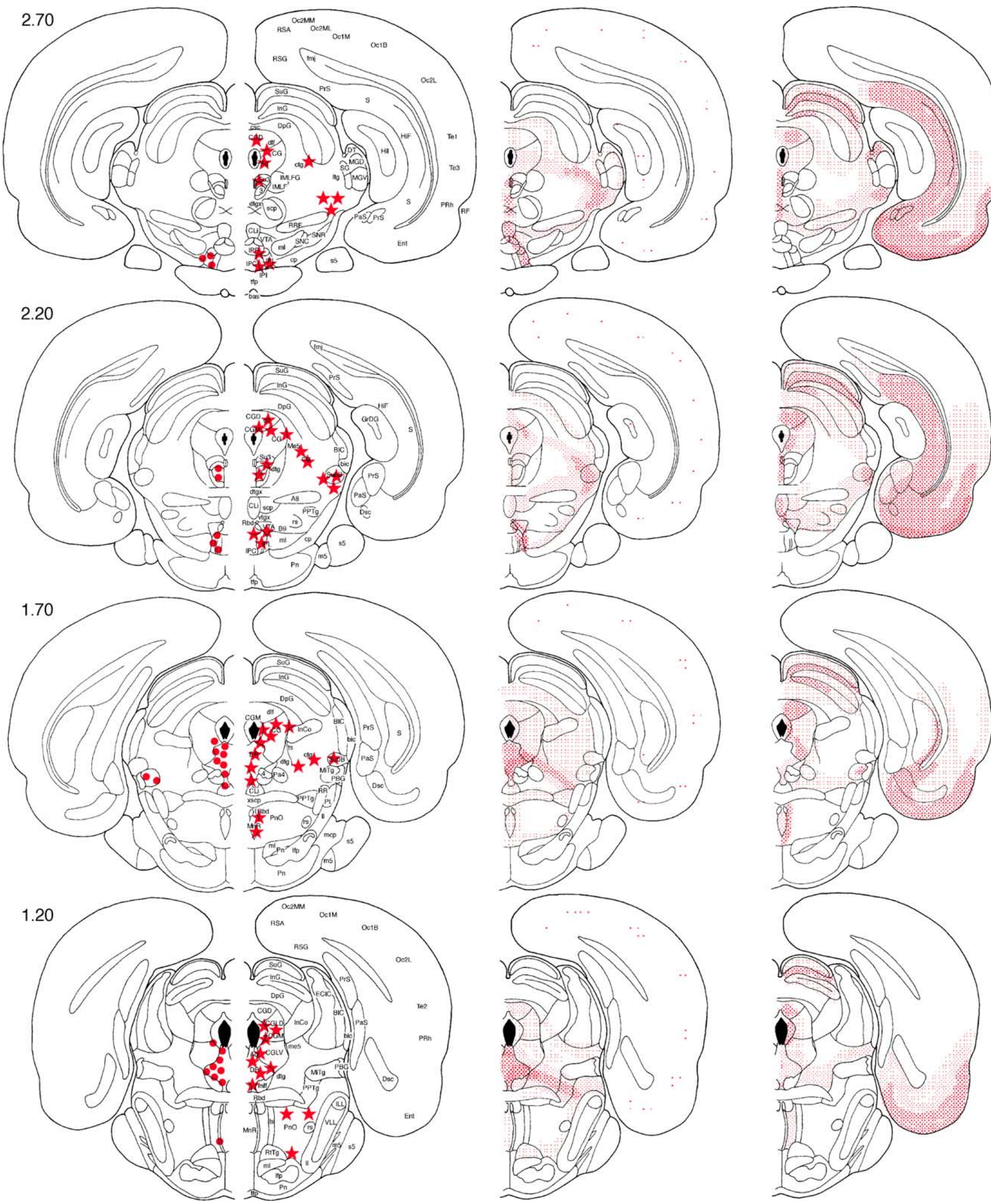

Figs. 1–9. (*Continued*)

monkey [76] contain dense binding sites. Projections to the cortex (prefrontal, insular), the medial thalamus, the hippocampus (subiculum) and the medial hypothalamus (ventromedial, premamillary, medial preoptic and anterior hypothalamic nuclei) which emanate from amygdaloid nuclei all contain prominent galanin receptor binding sites. Rostral projections from the central amygdaloid nucleus (bed nucleus of the stria terminalis) and caudal projections (ventral tegmental area, substantia nigra compacta, peripeduncular nucleus, reticular formation, dorsal raphe,

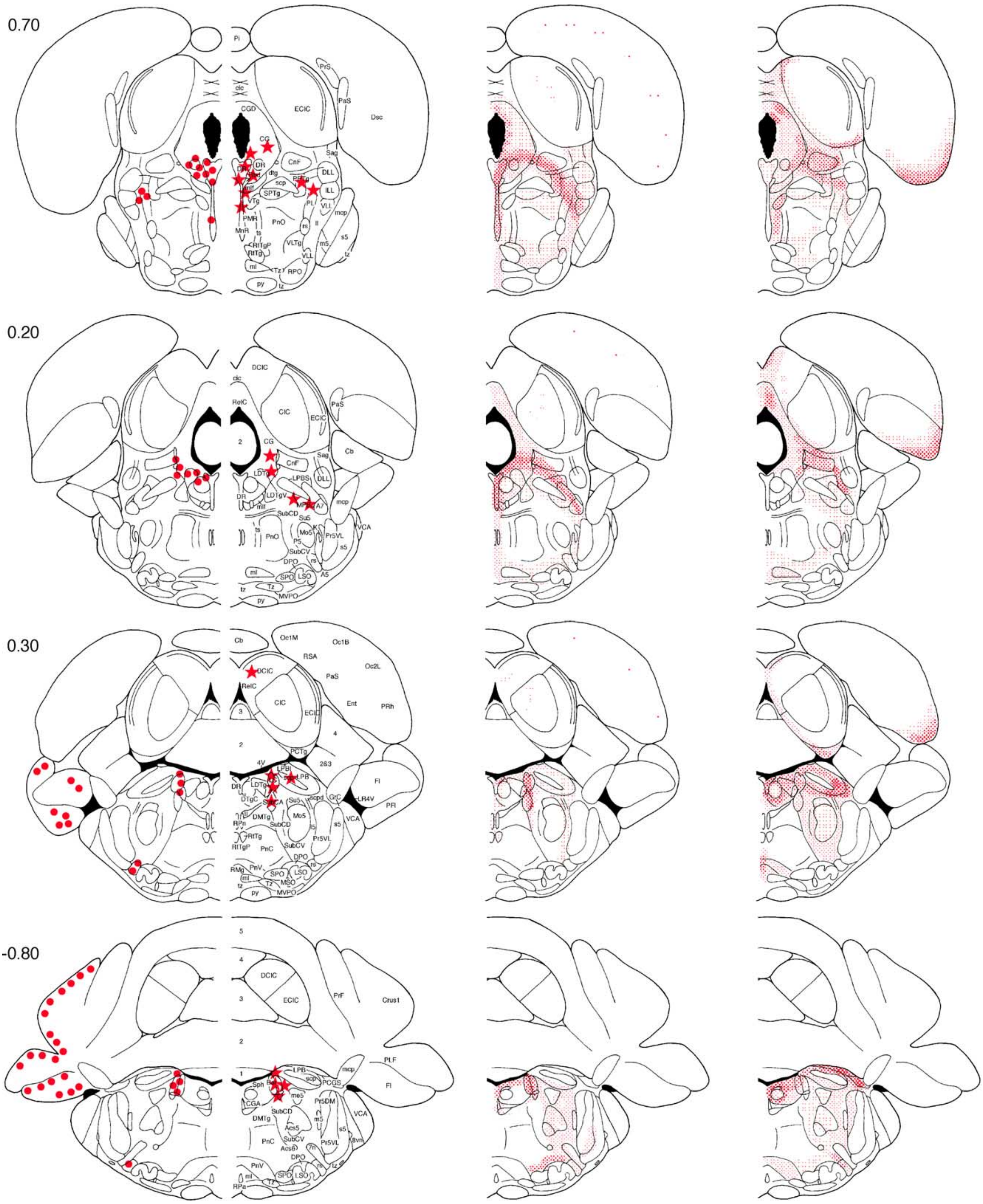

Figs. 1–9. (*Continued*)

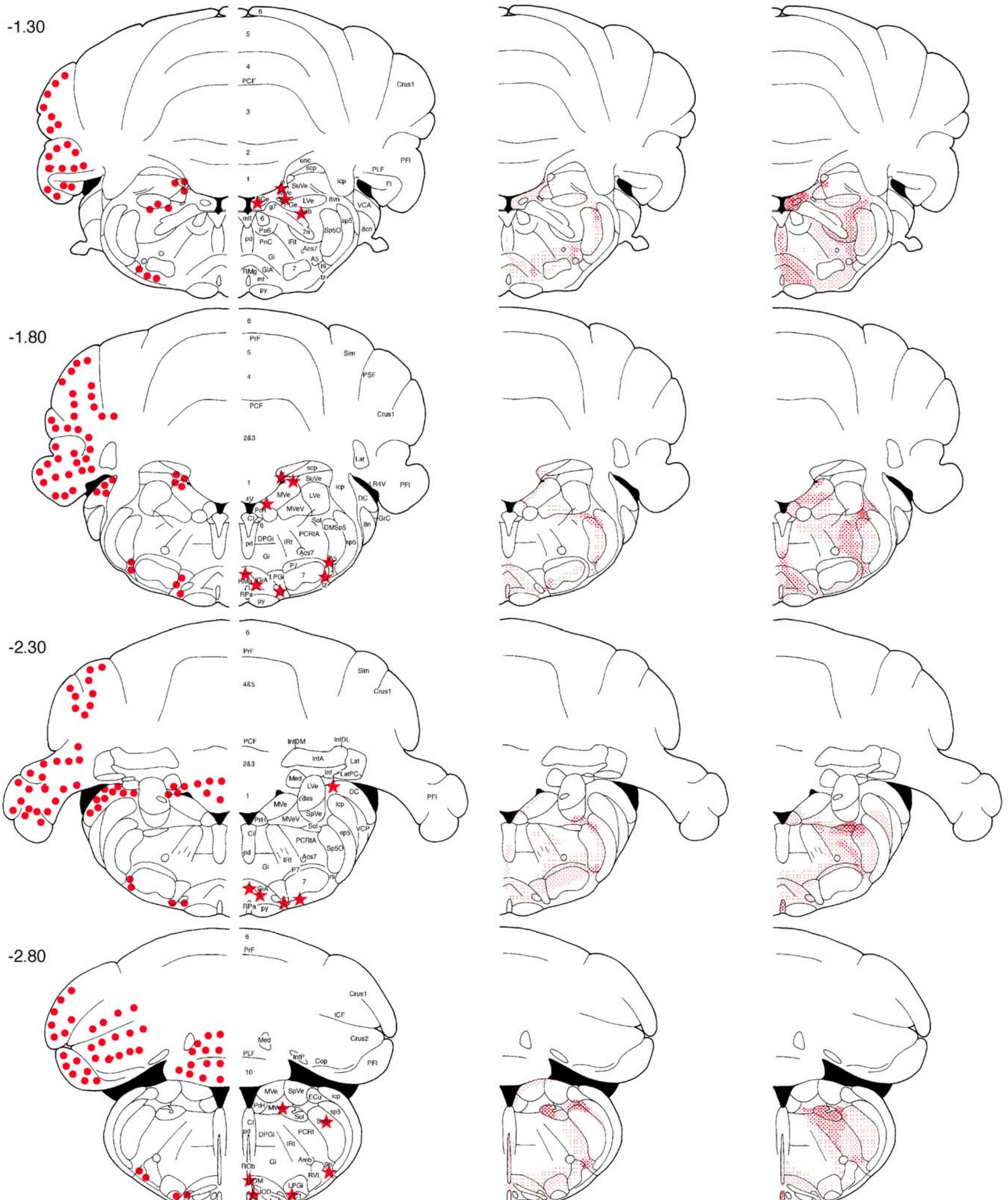

Figs. 1–9. (*Continued*)

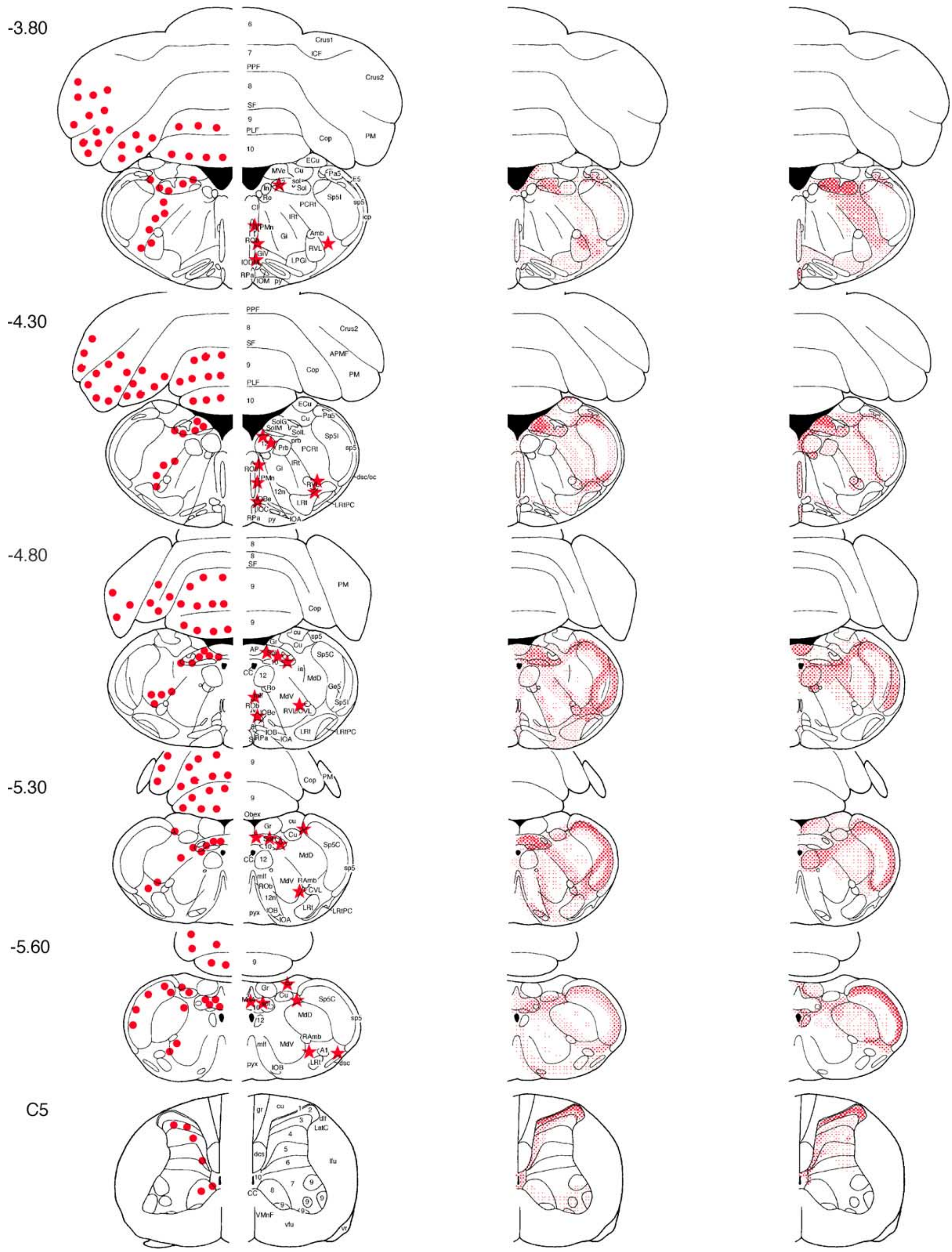

Figs. 1–9. (*Continued*).

central gray, parabrachial nuclei) all contain an appreciable concentration of binding sites. Very dense galanin binding noted in the stria terminalis constitutes a possible pathway for amygdala axons containing galanin receptors. The possibility of galanin-containing receptor-binding axons in the stria terminalis suggests the presence of autoreceptors.

The dense appearance of galanin binding sites in the sensory terminal areas of the medulla and the spinal cord where galanin is colocalized with other sensory neuropeptides, e.g.,

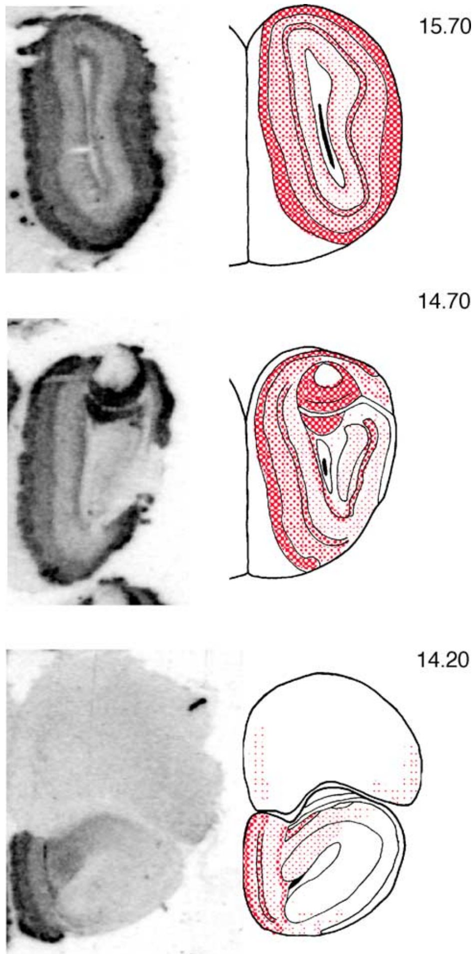

Fig. 10. Autoradiographic image and corresponding schematical drawings of the most anterior olfactory regions of the rat brain showing extremely dense galanin receptor accumulations in areas which exhibit only very sparse or are devoid of any substantial innervation with galanin immunoreactive nerves.

substance P and calcitonin gene-related peptide [19,27,40], suggests a heavy involvement of galanin in the modulation of sensory nociceptive information.

4. Coexistence with other neurotransmitter systems

The widespread distribution of galanin-ir within the central nervous system suggest the multiple coexistence of this peptide with several other neurotransmitters and neuropeptides. There is increasing interest in coexisting neurotransmitters, since there are functional indications that neuronal signaling can be modulated by cocontained substances.

4.1. Galanin in cholinergic neurons—galanin-ir and choline acetyltransferase-ir or acetylcholinesterase-ir

The coexistence of galanin-ir with choline acetyltransferase (ChAT)-ir has been shown in somata of the septum-basal forebrain complex projecting to the hippocampus in the rat [62]. A large number of cholinergic neurons of the medial septal nucleus and the diagonal band also stained positive for galanin-ir but it was not seen in all cholinergic neurons of the basal forebrain. For example, although the nucleus basalis of Meynert has been shown to give rise to a cholinergic projection to the hippocampus [32,64], it did not contain galanin-ir. True blue injections into the ventral part of the hippocampus resulted in retrograde staining of galanin-ir and ChAT-ir neurons in the medial septal nucleus and the ventral portion of the diagonal band, whereas dye injection into the dorsal part of the hippocampus did not reveal galanin-ir cells in the forebrain. Three different morphological types of galanin-ir fibers in the rat hippocampus were described [63]: (a) a fine galanin-ir network of fibers in most parts of the hippocampal formation; (b) coarse, strongly immunoreactive fibers in the strata radiatum and oriens of the ventral CA3 region; (c) fine punctate fibers mainly within the granule cell layers and the pyramidal cell layer. Lesion studies of different afferent pathways to the hippocampus show that these fibers belong to cholinergic and catecholaminergic projections [63]. Among cholinergic projections, the authors revealed, there are two pathways for cholinergic fiber projections to the hippocampus: the largest inputs to the hippocampus are contained in the dorsal pathways (dorsal fornix, fimbria and supracallosal striae), whereas there seems to be another minor subcortical ventral pathway of cholinergic neurons from the diagonal band nucleus. Transsection of the dorsal pathways resulted in the almost complete disappearance of fine galanin-ir fibers in the dorsal portion of the hippocampal formation but were spared in the more ventral sections. Coarse fibers were almost completely abolished throughout the dorsal hippocampal formation, as was the fine punctate fiber population. As a result of dorsal pathway lesions, cell bodies of the diagonal band had a retrograde accumulation of galanin-ir material. Transsection of the ventral pathway resulted in a depletion of the fine galanin-ir fibers seen in the ventral planes of the hippocampal formation, while only slightly influencing them at dorsal levels. Coarse fibers were not affected and galanin-ir puntate fibers were slightly depleted in the most ventral planes. As a result of the ventral transsection few cell bodies of the lateral aspects of the diagonal band nucleus showed a build-up of galanin-ir material. Ibotenic acid lesions of the medial septum and the diagonal band caused small decreases in fine galanin-ir fibers adjacent to pyramidal and granule cell layers. However, no effect on coarse fibers was seen.

Essentially, all AChE-staining cell bodies within the medial septal nucleus, the diagonal band and the nucleus basalis (substantia innominata) were shown to cocontain galanin-ir in the owl monkey. In the hippocampus and the dentate gyrus AChE-containing fibers appeared to contain galanin-ir [61]. A more extensive coexistence of the cholinergic forebrain projection to the hippocampus was shown to exist in the owl monkey compared with the rat. The authors suggest that this signified a greater functional significance to forebrain cholinergic–galanin interaction in higher animals.

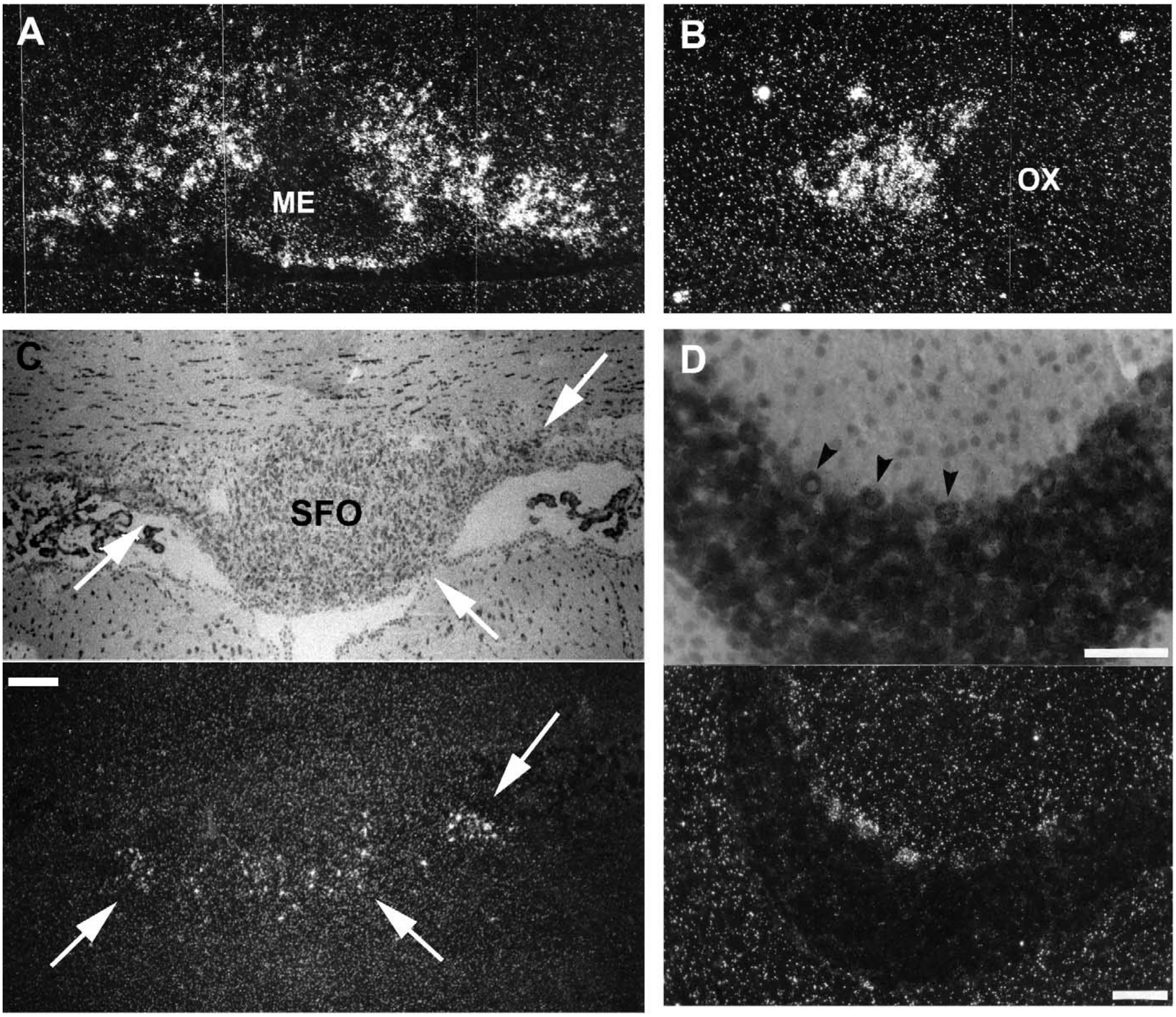

Fig. 11. Darkfield photomicrographs of galanin mRNA containing neurons in: (A) the arcuate nucleus next to the median eminence (ME; level 6.70); (B) the supraoptic nucleus next to the optic chiasm (OX). Part (C) shows a brightfield image of the subfornical organ (SFO; upper part), arrows indicate the position of galanin mRNA containing neurons visible in the darkfield photomicrographs (lower part). Part (D) shows a brightfield enlargement of the cerebellum (upper part), arrows indicate Purkinje cells containing galanin mRNA as shown in the darkfield photomicrographs (lower part).

The coexistence of galanin-ir in cholinergic neurons of the septum-basal forebrain complex projecting to the hippocampus seems to be important with respect to a possible participation in Alzheimer's disease, which has been shown to involve degeneration of cholinergic septal-basal forebrain neurons and loss of cholinergic input to the hippocampus [62].

4.2. Galanin in catecholaminergic neurons—galanin-ir and tyrosine hydroxylase-ir

Galanin-ir was found to coexist with tyrosine hydroxylase-ir (TH-ir) in several areas of the rat brain, e.g., the arcuate nucleus [17,60] (the so-called A12 TH cell groups, according to Dahlström and Fuxe [11] and Hökfelt et al. [24,25]). Coexistence of galanin-ir and TH-ir was also observed at the base of the brain lateral to the ventromedial nucleus. A few cells showing coexistence were also found in the dorsolateral aspects of the ventromedial nucleus [60]. The A6 (locus coeruleus) and the A4 TH cell groups contained the highest numbers of coexisting cells. In addition, the A1 TH cell groups located dorsolateral to the lateral reticular nucleus mostly contained galanin-ir [60]. No evidence was found, however, that the C1 adrenaline cell group coexisted with TH-ir were also found in the dorsal vagal complex [60]. There was no evidence that galanin was colocalized within phenylethanolamine-*N*-methyltranserase-ir (PNMT-ir) adrenergic cells, e.g., in the C1 cell group close to the ambiguous nucleus [49,60].

Galanin coexistence in noradrenergic neurons was described in a study whereby the immunoreactivity of galanin and DBH was coupled to axonal transport techniques in order to demonstrate afferent inputs into the paraventricular nucleus. Galanin was found to coexist with DBH-ir in A1, A6 (locus coeruleus) and the dorsomedial hypothalamic nucleus which projected to the paraventricular nucleus [49]. Galanin-ir and DBH-ir doubly labeled cells which projected to the paraventricular nucleus were also found in the lateral hypothalamic area, the arcuate nucleus and the medial preoptic area.

Knife-cut lesion studies [63] revealed that after transsection of the dorsal (noradrenergic) bundle galanin-ir fine fibers were almost completely depleted in the hippocampal formation, with the exception of fine fibers in proximity to the pyramidal and granule cell layers (contained in cholinergic fibers). Coarse and punctate fibers in the hippocampus appeared to be unaffected, with the exception of the most lateral area of the dentate gyrus, where the normally dense fine punctate fibers seemed to be depleted. Therefore, most of the fine galanin-ir fibers in the hippocampus appear to originate from the locus coeruleus and thus coexist with norepinephrine. These fibers reach the hippocampus primarily through the supracallosal striae, fimbria and ventral route just lateral and caudal to the diagonal band. It is intriguing that a classical dual innervation of cholinergic and adrenergic nerves to the hippocampus both coexist with galanin. In addition, many dorsal raphe cells which contain both 5-HT-ir and galanin-ir somata project nerve fibers to the hippocampus [60].

4.3. Galanin coexisting with GABA—galanin-ir and glutamic acid decarboxylase-ir (GAD-ir)

Galanin-ir was also found to coexist with glutamic acid decarboxylase-ir (GAD-ir) [58] in the posterior levels of the arcuate nucleus and the external layers of the median eminence. The tuberal and caudal magnocellular nuclei of the hypothalamus also contained both galanin-ir and GAD-ir. However, compared with GAD-ir neurons, galanin-ir neurons were sparse. True blue injection into the occipital cortex revealed that some of the galanin-ir neurons of the caudal magnocellular nucleus of the mamillary body project to the occipital cortex.

4.4. Galanin coexisting with other biogenic amines—galanin-ir and serotonin—galanin-ir and histidine decarboxylase-ir (HD-ir)

Most major nuclei containing serotonin-ir (5-HT-ir) also contained galanin-ir [60]. A large portion of the dorsal raphe and ventrally located mesencephalic somata contained galanin-ir and 5-HT-ir, as did the raphe obscurus and pallidus. Double staining was also seen at the nerve fiber level in the hippocampal formation, particularly in the granule cell layer of the gyrus dentatus.

The rat tuberomamillary nucleus cells were shown to contain both galanin-ir and HD-ir, which is used as a marker for histamine-containing neurons [43]. Fast blue injections and retrograde labeling has shown that the cells of the tuberomamillary nucleus also project to the ventral hippocampus [43].

4.5. Galanin coexisting with neuropeptides—galanin-ir and vasopressin-ir (VP-ir)

Palkovits et al. [74] studied the origin of the galanin-ir fibers in the hypothalamo–hypophyseal system and found galanin-ir cell bodies which projected to the internal layer of the median eminence and the posterior pituitary located in the supraoptic, magnocellular paraventricular and accessory magnocellular nuclei. The coexistence of galanin-ir and VP-ir has been demonstrated within the majority of magnocellular neurons of the hypothalamic paraventricular nucleus and also within a considerable number of parvocellular neurons [60,78,90], in addition to the accessory magnocellular cells of the lateral hypothalamus and the supraoptic nucleus [78,90]. This is of special interest, as the neuronal distribution of the galanin-ir and VP-ir nerves in the posterior part of the pituitary seems to completely overlap. Furthermore, depletion of both peptides from the posterior pituitary following water deprivation and salt loading has been demonstrated [90]. Rökaeus et al. [78], using in situ hybridization, found levels of mRNA encoded preprogalanin elevated in the paraventricular and supraoptic nuclei of Brattleboro (diabetes insipidus) rats, but RIA levels of galanin decreased in the posterior pituitary. The authors suggested that in Brattleboro rats the production and secretion of galanin are enhanced.

4.6. Galanin-ir and cholecystokinin-ir (CCK-ir)

A system of spinothalamic neurons containing both galanin-ir and CCK-ir has been identified [41]. Cell bodies of this system are located in the lumbar segments of the spinal cord at levels L1–L5. They are preferentially localized dorsal and lateral to the central canal. These cells send processes via the ventral part of the lateral funiculus to the caudal thalamus. Transsection experiments and retrograde labeling indicated that the spinothalamic galanin–CCK-ir projection represents a crossed pathway. This fiber bundle appeared to traverse the region dorsal to the lemniscus medialis and medially at the level of the fasciculus retroflexus and could be traced back to the central gray at the level of the dorsal raphe. Skofitsch and Jacobowitz [88] reported that this long oblique dorsolateral projection was reminiscent of the dorsal and ventral noradrenergic pathways described previously [28,29,36,73]. It was therefore suggested that this pathway contained noradrenergic–galanin coexisting processes from the locus coeruleus and A4 somata in addition to possible ventral projections from the A1, A2 and C1 cells cocontained with galanin. At the posterior ventral thalamus level, Ju et al. [40] presented evidence that the galanin–CCK pathway disappeared after complete transsection of the spinal cord, thus indicating that this projection emanates from cells in the spinal cord. However, the possibility that spinal lesions result in the destruction of sensory inputs to monoaminergic cell groups, thereby resulting in the reduction of mRNA required for peptide synthesis, should not be overlooked.

4.7. Multiple coexistence of galanin-ir—galanin-ir and sensory neuropeptides

Galanin-ir was found to be contained in capsaicin-sensitive primary afferent C-fibers in the medulla oblongata and the spinal cord of rats [6,86]. Among the variety of neuropeptides in these areas which are sensitive to capsaicin—e.g., substance P, neurokinin A, cholecystokinin, somatostatin, vasoactive intestinal polypeptide, corticotrophin releasing factor, calcitonin gene-related peptide (for review, see [84])—galanin-ir was found to be colocalized with substance P (SP) and/or calcitonin gene-related peptide (CGRP) within the same cells of the dorsal horn ganglion of pig [19] and rat [40]. CGRP was previously found to be localized in large-diameter motor neurons (type A cells) and together with SP-ir in small-diameter type B cells that belong to primary sensory afferents [84]. Virtually all SP-ir neurons were found to contain CGRP-ir. Recently it was demonstrated that almost all of the comparatively few galanin-ir neurons in the dorsal root ganglia also contain SP-ir and CGRP-ir [19,40]. This multiple coexistence is of special interest in view of the generation of nociceptive impulses from primary sensory neurons.

4.8. Galanin-ir, TH-ir and growth hormone releasing factor-ir (GRF-ir)

The coexistence of galanin-ir and TH-ir in neurons of the anterior arcuate nucleus has been reported [17]. Some of these neurons also seem to cocontain GRF-ir, which is of special interest in view of the capability of galanin to release growth hormone from the anterior pituitary in man and rat [1,57,65,71]. Murakami et al. [65] presented evidence which suggests that galanin-induced GH secretion is at least partly mediated by GRF.

5. Physiology and behavior

Galanin as a multi-functional neuropeptide [23]—galanin alters the release of several neurotransmitters:

1. Inhibition of release of acetylcholine in the hippocampus [18].
2. Regulation of the release of biogenic amines in the hypothalamus [57].
3. Release of growth hormone [2,3,5,57,65,71].
4. Release of prolactin [45,57].
5. Release of luteinizing hormone in the steroid-primed ovariectomized rat [79].

Chan-Palay [4] first observed a hyperinnervation of galanin fibers in the human basal forebrain of Alzheimer's disease patients. This suggests a possible role for galanin in the cholinergic dysfunction characteristic of this disease.

Galanin also has been thought to be involved in other neuronal functions such as learning and memory [100], epileptic activity [54–56] nociception [50], spinal reflexes and feeding [46–48].

Wrenn and Crawley [100] reviewed the pharmacological evidence supporting a role for galanin in cognition and affect:

1. Galanin is localized in brain pathways involved in both cognition and affect.
2. Galanin has inhibitory actions on a variety of memory tasks including the Morris water maze, delayed nonmatching to position, T-maze delayed alternation, starburst maze, passive avoidance, active avoidance, and spontaneous alternation.
3. Galanin may inhibit learning and memory by inhibiting neurotransmitter release and neuronal firing rate.
4. Two signal transduction mechanisms through which galanin exerts its inhibitory actions are the inhibition of phosphatidyl inositol hydrolysis and the inhibition of adenylate cyclase.
5. Galanin released during periods of burst firing from noradrenergic locus coeruleus terminals in the ventral tegmental area (VTA) may lead to symptoms of depression through inhibition of dopaminergic VTA neurons.
6. Intraventricular galanin has anxiolytic effects in a punished drinking test. Intra-amygdala galanin has anxiogenic effects in a punished drinking test.

The recent production of galanin knockout and overexpressing transgenic mice has resulted in new insights into the physiological actions of this peptide [101]. These initial studies have provided evidence that galanin acts as a developmental and trophic factor to subsets of neurons in the nervous and neuroendocrine systems. Fewer cholinergic basal forebrain neurons and memory deficits were observed in galanin knockout mice, whereas mice overexpressing galanin display hyperinnervatin of basal forebrain and memory deficits [9,10,94]. Recent work on galanin receptor subtype (GAL-R1) in mice with a null mutation in the galanin-R1 gene has revealed that galanin exerts anxiolytic actions under conditions of relatively high stress [26].

An intriguing hypothesis has been put forward by Weiss et al. [99]. They describe a "hypothesis that attempts to account for how changes in noradrenergic systems in the brain can affect depression-related behaviors and symptoms. It is hypothesized that increased activity of the locus coeruleus (LC) neurons, the principal norepinephrine (NE)-containing cells in the brain, causes release of galanin in the ventral tegmental area (VTA) from LC axon terminals in which galanin is colocalized with NE. It is proposed that galanin release in VTA inhibits the activity of dopaminergic cell bodies in this region whose axons project to forebrain, thereby resulting in two of the principal symptoms seen in depression, decreased motor activation and decreased appreciation of pleasurable stimuli (anhedonia). The genesis of this hypothesis, which derives from studies using an animal model of depression is described as well as recent data consistent with the hypothesis. The formulation proposed suggests that galanin antagonists may be of therapeutic benefit in the treatment of depression."

Harro and Oreland [21] also implicate the locus coeruleus in their speculative discourse concerning depression as a spreading adjustment disorder of monoaminergic neurons. They suggest that the "primary defect emerges in the regulation of firing rates in brainstem monoaminergic neurons, which brings about a decrease in the tonic release of neurotransmitters in their projection areas, an increase in postsynaptic sensitivity and concomitantly, exaggerated responses to acute increases in the presynaptic firing rate and transmitter release." Prior work has revealed that the central gray-containing dorsal raphe cells and ventral tegmental area are innervated by fibers that arise from the locus coeruleus and the ventral noradrenergic pathway [53,77]. Therefore it is reasonable to suggest that dysregulation of the locus coeruleus and hindbrain noradrenergic cells may lead in turn to dysregulation of serotonergic and dopaminergic neurotransmission. In this regard it is interesting that there is frequently locus coeruleus neuronal degeneration in Parkinson's disease. Parkinson's patients are oftentimes diagnosed with depression.

It was also suggested that dysregulation of neuropeptides, neuropeptide Y, substance P and galanin, peptides that are contained within the locus coeuleus or in close proximity [96], may reinforce the locus coeruleus dysfunction and thus further weaken the adaptivity to stressful stimuli.

We would suggest that a noradrenergic–dopaminergic interaction also results from noradrenergic nerves which emanate from the ventral catecholaminergic pathway. Cell bodies responsible for this projection emanate from the cells in the hindbrain (nucleus of the solitary tract, lateral reticular nucleus) [73]. These nuclei contain dense clusters of galanin immunoreactive cells and a very dense innervation of galanin-containing fibers. The nucleus of the solitary tract (nucleus tractus solitarii, also known as the A2 cell group) and the lateral reticular nucleus (which contains the A1 noradrenergic neurons) colocalized with tyrosine hydoxylase [60] and DBH was found to coexist with galanin in the A1 cells.

The ventral bundle is the "pipeline" of the noradrenergic axons that emanate from A1 and A2 norepinephrine-containing neurons of the hindbrain [28,29,37]. The more rostral dorsal bundle carries the A6-locus coeruleus axons. Galanin-containing fibers were observed in the region of the ventral noradrenergic bundle. Transection of the noradrenergic ventral bundle produced changes in dopaminergic systems suggesting a noradrenergic–dopaminergic interaction. Unilateral ventral bundle transection increased dopamine concentrations in the substantia nigra and ventral tegmental area [67]. These results indicate a broad projection field for the noradrenergic ventral bundle and suggest a noradrenergic–dopaminergic interaction.

6. Conclusion and future trends

After a decade of mapping the localization of a variety of CNS neuropeptides [34,35,68,69,81–83,85,87–89,91,93,96], it has become evident that because of the ubiquitous localization of the cells and fiber plexuses, a single function cannot be attributed to any one peptide. When receptor binding sites for peptides have been mapped (see e.g., [85,87,90]), there is generally observed a good correlation with the immunocytochemical distribution of nerve fibers, except for occasional mismatches [22]. The presence of nerves and binding sites in brain areas with established functions implicates a role for the peptides in these regions. For lack of detailed information regarding peptidergic mechanisms of action, it has been reasonable to suggest a broad generalization that neuropeptides somehow 'modulate' a variety of behavioral activities in the brain.

Several studies have uncovered the functional role of galanin in the central nervous system. The observation that galanin coexists with acetylcholine in septal–basal forebrain neurons which project to the hippocampus has implicated this peptide in the release of acetylcholine from the ventral hippocampal areas [18,61,62]. This poses the question of involvement of galanin in Alzheimer's disease [3]. In the hypothalamus–median eminence complex, galanin has been implicated in the release mechanism of growth hormone and prolactin from the anterior pituitary, in addition to hypothalamic involvement in feeding behavior [3,5,45,46,57,65,71]. The presence of galanin in the primary sensory neurons in the spinal cord appears to be involved in influencing nociceptive impulses [6,19,40,42,51,52, 59,87,88,91].

An approach to the study of peptide function is to learn about the dynamics of neuropeptide biosynthesis. This can be accomplished by the use of hybridization histochemistry [98]. Generally, but with some exceptions, neuropeptide mRNA in situ hybridization results match the localization of peptide somata observed by immunocytochemistry. However, quantitative autoradiography is very useful for the examination of neuropeptide gene expression in the central nervous system. In particular, in situ hybridization histochemistry has its greatest usefulness in its ability to obtain an index of peptide biosynthesis at the level of the single neuron or cell group. Physiological or pharmacological manipulations reveal alterations in gene expression [95].

Because of the widespread localization of neuropeptide cell body groupings (nuclei) in the CNS, it is likely that they are innervated by different afferent inputs. The regulation of the synthesis of the peptides (gene expression) at different brain regions is probably influenced by these neural inputs in addition to the effects of circulating hormones. Therefore, a meaningful pursuit of the dynamics of peptides and other neurochemicals is at the discrete brain level studies by histochemical means.

List of abbreviations

10	Dorsal motor nucleus of the vagus	−3.72 to −5.50
12	Hypoglossal nucleus	−3.72 to −5.60
12n	Root of hypoglossal nerve	−3.72 to −5.30
2n	Optic nerve	10.20–9.20
3	Oculomotor nucleus	2.96–1.96
3n	Oculomotor nerve or its root	3.40–2.96
3PC	Oculomotor nucleus, parvocellular part	2.96–1.96
3V	3rd ventricle	9.20–4.20
4	Trochlear nucleus	1.70
4n	Trochlear nerve or its root	3.20–0.70
4V	4th ventricle	−0.16 to −4.30
4x	Trochlear decussation	−0.16 to −0.30
6	Abducens nucleus	−1.04 to −1.80
6n	Root of abducens nerve	−0.16 to −1.52
7	Facial nucleus	−1.30 to −2.60
7n	Facial nerve or its root	−0.68 to −1.30
8cn	Cochlear root of the vestibulocochlear nerve	−1.04 to −1.30
8Gn	Vestibulocochlear ganglion	−1.30
8n	Vestibulocochlear nerve	−1.80 to −2.60
8vn	Vestibular root of the vestibulocochlear nerve	−0.68 to −1.52
9n	Glossopharyngeal nerve	−2.80
A1	A1 noradrenaline cells	−4.68 to −5.30
A2	A2 noradrenaline cells	−5.08 to −5.30
A4	A4 noradrenaline cells	−1.52 to −2.30
A5	A5 noradrenaline cells	0.28 to −2.00
A7	A7 noradrenaline cells	0.28–0.20
A8	A8 dopamine cells	2.28–1.96
AA	Anterior amygdaloid area	8.20
AAD	Anterior amygdaloid area, dorsal part	8.08–7.60
AAV	Anterior amygdaloid area, ventral part	8.08–7.60
AC	Anterior commissural nucleus	8.20–8.08
ac	Anterior commissure	8.74–8.60
aca	Anterior commissure, anterior part	12.20–9.20
Acb	Accumbens nucleus	11.70
AcbC	Accumbens nucleus, core	11.20–9.70
AcbSh	Accumbens nucleus, shell	11.20–9.70
Acc	Accessory neurosecretory nuclei	6.88
aci	Anterior commissure, intrabulbar part	14.20–12.70
ACo	Anterior cortical amygdaloid nucleus	8.08–6.20
acp	Anterior commissure, posterior part	8.74–8.08
Acs	Accessory nucleus of the ventral horn	C1–C5
Acs5	Accessory trigeminal nucleus	−0.68 to −0.80
Acs6	Accessory abducens nucleus	−0.80
Acs7	Accessory facial nucleus	−1.30 to −2.30
AD	Anterodorsal thalamic nucleus	7.70–6.88
AF	Amygdaloid fissure	5.40–2.96
AHA	Anterior hypothalamic area, anterior part	7.70–7.60

AHC	Anterior hypothalamic area, central part	7.20
AHiAL	Amygdalohippocampal area, anterolateral part	5.40–4.70
AHiPM	Amygdalohippocampal area, posteromedial part	4.84–2.96
AHP	Anterior hypothalamic area, posterior part	6.88–6.70
AI	Agranular insular cortex	14.70–7.70
AL	Nucleus of the ansa lenticularis	6.70
al	Ansa lenticularis	7.20–5.70
alv	Alveus of the hippocampus	6.88–2.96
AM	Anteromedial thalamic nucleus	7.70–6.88
Amb	Ambiguus nucleus	−2.60 to −4.80
AMPO	Anterior medial preoptic nucleus	8.74–8.60
Ang	Angular thalamic nucleus	6.44–6.20
AOB	Accessory olfactory bulb	15.20–14.20
AOD	Anterior olfactory nucleus, dorsal part	14.20–13.20
AOE	Anterior olfactory nucleus, external part	15.20–14.20
AOL	Anterior olfactory nucleus, lateral part	15.20–13.20
AOM	Anterior olfactory nucleus, medial part	14.20–12.70
AOP	Anterior olfactory nucleus, posterior part	12.20–11.70
AOV	Anterior olfactory nucleus, ventral part	14.20–12.70
AP	Area postrema	−4.68 to −5.08
APir	Amygdalopiriform transition area	4.84–2.96
APMF	Ansoparamedian fissure	−4.24 to −4.80
APTD	Anterior pretectal nucleus, dorsal part	4.84–3.70
APTV	Anterior pretectal nucleus, ventral part	4.48–3.70
Aq	Aqueduct(Sylvius)	3.80–0.70
ar	Acoustic radiation	4.70–4.48
Arc	Arcuate hypothalamic nucleus	6.88–4.48
asc7	Ascending fibers of the facial nerve	−2.30
AStr	Amygdalostriatal transition area	7.20–5.40
Atg	Anterior tegmental nucleus	1.36–1.00
AV	Anteroventral thalamic nucleus	8.08
AVDM	Anteroventral thalamic nucleus, dorsomedial part	7.70–7.20
AVPO	Anteroventral preoptic nucleus	8.74–8.60
AVVL	Anteroventral thalamic nucleus, ventrolateral part	7.70–7.20
B	Basal nucleus of Meynert	8.20–5.86
B9	B9 5-hydroxytryptamine cells	2.20–1.96
BAC	Bed nucleus of the anterior commissure	8.20
BAOT	Bed nucleus of the accessory olfactory tract	7.20–6.70
Bar	Barrington’s nucleus	−0.16 to −0.80
bas	Basilar artery	2.70 to −2.60
BIC	Nucleus of the brachium of the inferior colliculus	2.28–1.00
bic	Brachium of the inferior colliculus	2.28–1.00
BLA	Basolateral amygdaloid nucleus, anterior part	7.20–5.70
BLP	Basolateral amygdaloid nucleus, posterior part	6.70–4.84
BLV	Basolateral amygdaloid nucleus, ventral part	6.88–5.70
BM	Basomedial amygdaloid nucleus	6.20–5.86
BMA	Basomedial amygdaloid nucleus, anterior part	6.88–6.44
BMP	Basomedial amygdaloid nucleus, posterior part	5.70–4.84
bp	Brachium pontis	2.28–1.00
bsc	Brachium of the superior colliculus	4.84–2.96
BST	Bed nucleus of the stria terminalis	9.48
BSTI	Bed nucleus of the stria terminalis, intermediate division	8.74–8.60
BSTIA	Bed nucleus of the stria terminals, intraamygdaloid division	6.44–5.20
BSTL	Bed nucleus of the stria terminals, lateral division	9.20
BSTLD	Bed nucleus of the stria terminals, lateral division dorsal part	8.74–8.60

BSTLJ	Bed nucleus of the stria terminalis, lateral division, juxtacapsular part	8.74–8.60
BSTLP	Bed nucleus of the stria terminalis, lateral division, posterior part	8.20
BSTLV	Bed nucleus of the stria terminalis, lateral division, ventral part	8.74–8.60
BSTMA	Bed nucleus of the stria terminalis, medial division, anterior part	9.20–8.60
BSTMPI	Bed nucleus of the stria terminalis, medial division, posterointermediate part	8.20–8.08
BSTMPL	Bed nucleus of the stria terminalis, medial division, posterolateral part	8.20–7.60
BSTMPM	Bed nucleus of the stria terminalis, medial division, posteromedial part	8.20–8.08
BSTS	Bed nucleus of the stria terminalis, supracapsular division	7.70–7.20
BSTV	Bed nucleus of the stria terminalis, ventral division	9.20–8.60
C1	C1 adrenaline cells	−2.60 to −5.08
C2	C2 adrenaline cells	−2.60 to −4.30
C3	C3 adrenaline cells	−2.60 to −3.80
CA1	Fields of Ammon's horn	7.20–2.20
CA2	Fields of Ammon's horn	7.20–2.20
CA3	Fields of Ammon's horn	7.20–2.20
CB	Cell bridges of the ventral striatum	10.00–9.20
Cb	Cerebellum	0.20 to −0.30
cc	Corpus callosum	9.48–4.48
CC	Central canal	−4.68 to C5
CeC	Central cervical nucleus	C1–C5
CeL	Central amygdaloid nucleus, lateral division	7.20–6.20
CeLC	Central amygdaloid nucleus, lateral division, capsular part	6.88–6.44
CeLCn	Central amygdaloid nucleus, lateral division, central part	6.88–6.44
Cem	Central amygdaloid nucleus, medial division	6.88–6.20
CeMAD	Central amygdaloid nucleus, medial division, anterodorsal part	6.88
CeMPV	Central amygdaloid nucleus, medial division, posteroventral part	6.88–6.44
cg	Cingulum	10.60–3.20
CG	Central (periaqueductal) gray	3.80–0.20
Cg1	Cingulate cortex, area 1	13.70–7.70
Cg2	Cingulate cortex, area 2	10.70–7.70
Cg3	Cingulate cortex, area 3	13.70–11.20
CGA	Central gray, alpha part	−0.68 to −0.80
CGD	Central gray, dorsal part	3.40–0.70
CGLD	Cenrtal gray, lateral dorsal part	1.36–1.00
CGLV	Central gray, lateral ventral part	1.36–1.00
CGM	Central gray, medial part	3.20–1.00
CGPn	Central gray of the pons	−0.68
ChP	Choroid plexus	−4.24
CI	Caudal interstitial nucleus of the medial longitudinal fasciculus	−1.80 to −3.80
CIC	Central nucleus of the inferior colliculus	0.20 to −0.68
cic	Commissure of the inferior colliculus	0.70–0.20
Cl	Claustrum	12.20–7.60
CL	Centrolateral thalamic nucleus	6.70–5.20
Cli	Caudal linear nucleus of the raphe	2.96–1.36
cll	Commissure of the lateral lemniscus	1.00–0.28
CM	Central medial thalamic nucleus	7.60–5.20
CnF	Cuneiform nucleus	0.70–0.20
Cop	Copula of the pyramis	−2.80 to −5.30
cp	Cerebral peduncle, basal part	5.20–1.96
CPu	Caudate putamen (striatum)	11.20–5.20
Crus1	Crus1 of the ansiform lobule	−0.68 to −3.80
Crus2	Crus2 of the ansiform lobule	−2.60 to −4.80
csc	Commissure of the superior colliculus	3.80–2.70
CST	Nucleus of the commmissural stria terminalis	8.60
cst	Commissural stria terminalis	7.20–6.20
ctg	Central tegmental tract	4.20–1.36

Cu	Cuneate nucleus	−3.72 to −5.60
cu	Cuneate fasciculus	−4.24 to −5.60
CVL	Caudoventrolateral reticular nucleus	−4.68 to −5.60
Cx	Cerebral cortex	−0.16 to −0.80
CxA	Cortex-amygdala transition zone	8.74–7.20
D3V	Dorsal 3rd ventricle	8.08–4.70
DA	Dorsal hypothalamic area	6.88–5.70
das	Dorsal acoustic stria	−2.00 to −2.30
DC	Dorsal cochlear nucleus	−1.30 to −2.60
DCIC	Dorsal cortex of the inferior colliculus	0.28 to −0.80
dcs	Dorsal corticospinal tract	C1–C5
DEn	Dorsal endopiriform nucleus	11.20–2.96
df	Dorsal fornix	8.74–4.20
DG	Dentate gyrus	7.20–2.20
DHC	Nucleus of the dorsal hippocampal commissure	6.88–6.44
dhc	Dorsal hippocampal commissure	7.20–3.70
DI	Dysgranular insular cortex	10.20–8.70
Dk	Nucleus of the Darkschewitsch	4.20–3.20
dlf	Dorsal longitudinal fasciculus	4.20–1.36
DLG	Dorsal lateral geniculate nucleus	5.40–3.70
DLL	Dorsal nucleus of the lateral lemniscus	0.70–0.20
DM	Dorsomedial hypothalmic nucleus	5.86–4.84
DMC	Dorsomedial hypothalamic nucleus, compact part	5.70
DMD	Dorsomedial hypothalamic nucleus, diffuse part	6.44–5.70
DMSp5	Dorsomedial spinal trigeminal nucleus	−1.52 to −3.80
DMTg	Dorsomedial tegmental area	−0.16 to −0.80
Do	Dorsal hypothalamic nucleus	5.86
DP	Dorsal peduncular cortex	12.20–11.20
DpG	Deep gray layer of the superior colliculus	2.96–1.00
DPGi	Dorsal paragigantocellular nucleus	−1.80 to −3.30
DpMe	Deep mesencephalic nucleus	3.80–1.96
DPO	Dorsal periolivary region	0.20 to −0.80
DpWh	Deep white layer of the superior colliculus	2.96–1.00
DR	Dorsal raphe nucleus	1.96 to −0.30
dr	Dorsal root of spinal nerve	C1–C5
Dsc	Lamina dissecans of the enthorhinal cortex	2.20–0.28
dsc	Dorsal spinocerebellar tract	−3.72 to −5.60
DT	Dorsal terminal nucleus of the accessory optic tract	2.96–2.70
DTg	Dorsal tegmental nucleus	−0.16 to −0.30
dtg	Dorsal tegmental bundle	3.80 to −0.20
DTgP	Dorsal tegmental nucleus, pericentral part	0.28 to −0.30
dtgx	Dorsal tegmental decussation	2.96–2.20
DTr	Dorsal transition zone	12.70
E	Ependyma and subependymal layer	15.70–11.70
E5	Ectotrigeminal nucleus	−3.72 to −3.80
ec	External capsule	10.70–4.48
ECIC	External cortex of the inferior colliculus	1.36 to −0.80
Ecu	External cuneate nucleus	−2.60 to −4.30
eml	External medullary lamina	7.20–5.20
EP	Entopeduncular nucleus	6.88–5.70
EPl	External plexiform layer of the olfactory bulb	15.70–14.20
ERS	Epirubrospinal nucleus	1.36
Eth	Ethmoid thalamic nucleus	4.48–4.20
EW	Edinger-Westphal nucleus	3.80–2.20
F	Nucleus of the fields of Forel	4.84–4.48
f	Fornix	8.74–4.48

FC	Fasciola cinereum	5.70–3.70
fi	Fimbria of the hippocampus	7.70–4.70
FL	Forelimb area of the cortex	10.20–7.70
Fl	Flocculus	−0.30 to −1.52
fmi	Forceps minor of the corpus callosum	11.70–10.60
fr	Fasciculus retroflexus	5.40–3.40
Fr1	Frontal cortex, area 1	12.70–5.70
Fr2	Frontal cortex, area 2	14.20–5.70
Fr3	Frontal cortex, area 3	12.70–10.70
FStr	Fundus striati	10.70–7.60
FVe	F cell gray of the vestibular complex	−3.30 to −3.72
G	Gelatinosus thalamic nucleus	7.20–5.86
g7	Genu of the facilal nerve	−1.30 to −2.00
gcc	Genu of the corpus callosum	10.60–9.70
Ge5	Gelatinous layer of the caudal spinal trigeminal nucleus	−4.80
Gem	Gemini hypothalamic nucleus	5.20–4.48
GI	Granular insular cortex	10.70–7.70
Gi	Gigantocellular reticular nucleus	−1.30 to −4.30
GiA	Gigantocellular reticular nucleus, alpha part	−1.30 to −2.60
GiV	Gigantocellular reticular nucleus, ventral part	−2.80 to −3.80
Gl	Glomerular layer of the olfactory bulb	15.70–14.70
GP	Globus pallidus	8.74–5.70
Gr	Gracile nucleus	−4.68 to −5.60
gr	Gracile fasciculus	C1–C5
GrA	Granular cell layer of the accessory bulb	15.20–14.70
GrC	Granular layer of the cochlear nuclei	−0.30 to −2.30
GrDG	Granular layer of the dentate gyrus	5.20–2.20
Gu	Gustatory thalamic nucleus	5.40–4.84
hbc	Habenular commissure	4.84–4.20
HDB	Nucleus of the horizontal limb of the diagonal band	9.70–7.60
HiF	Hippocampal fissure	5.86–1.96
Hil	Hilus of the dentate gyrus	5.20
HL	Hindlimb area of the cortex	8.70–5.70
I	Intercalated nuclei of the amygdala	8.20–7.20
I5	Intertrigeminal nucleus	−0.16 to −0.68
ia	Internal arcuate fibers	−4.80 to −5.08
IAD	Interanterodorsal thalamic nucleus	7.70–7.60
IAM	Interanteromedial thalamic nucleus	7.20–6.70
IBl	Inner blade of the dentate gyrus	4.84–4.70
ic	Internal capsule	8.74–4.48
ICF	Intercrural fissure	−2.60 to −3.80
ICj	Islands of Calleja	11.70–8.60
ICjM	Islands of Calleja, major island	10.20–9.70
icp	Inferior cerebellar peduncle (restiform body)	−1.0 to −3.80
IF	Interfascicular nucleus	3.80–3.40
IG	Indusium griseum	10.70–4.48
IGL	Intergeniculate leaf	4.84–4.20
IGr	Internal granular layer of the olfactory bulb	15.70–14.20
II	Intermediate interstitial nucleus of the medial longitudinal fasciculus	−0.30 to −0.80
IL	Infralimbic cortex	12.20–11.20
ILL	Intermediate nucleus of the lateral lemniscus	1.20–0.70
IM	Intercalated amygdaloid nucleus, main part	6.88
IMA	Intramedullary thalamic area	4.84–3.70
IMD	Intermediodorsal thalamic nucleus	6.70–5.20
IMG	Amygdaloid intramedullary gray	6.88–6.44
iml	Internal medullary lamina	6.88–5.70

IMLF	Interstitial nucleus of the medial longitudinal fasciculus	4.20–2.70
IMLFG	Interstitial nucleus of the medial longitudinal fasciculus, greater part	3.80–2.70
imvc	Intermedioventral thalamic commissure	5.70
In	Intercalated nucleus of the medulla	−3.72 to −3.80
InCo	Intercollicular nucleus	1.70–1.00
Inf	Infracerebellar nucleus	−2.00 to −2.30
InfS	Infundibular stem	5.40–4.84
InG	Intermediate gray layer of the superior colliculus	3.40–1.00
InM	Intermedius nucleus of the medulla	−4.68
IntA	Interposed cerebellar nucleus, anterior part	−1.80 to −2.60
IntDL	Interposed cerebellar nucleus, dorsolateral part	−2.30
IntDM	Interposed cerebellar nucleus, dorsomedial part	−2.30
IntG	Intermediate geniculate nucleus	4.20
IntP	Interposed cerebellar nucleus, posterior part	−2.60 to −2.80
InWh	Intermediate white layer of the superior colliculus	3.40–1.00
IOA	Inferior olive, subnucleus A of the medial nucleus	−4.24 to −5.30
IOB	Inferior olive, subnucleus B of the medial nucleus	−4.24 to −5.60
IOBe	Inferior olive, beta nucleus	−4.24 to −4.80
IOC	Inferior olive, subnucleus C of the medial nucleus	−4.24 to −5.08
IOD	Inferior olive, dorsal nucleus	2.80 to −4.80
IODM	Inferior olive, dorsomedial cell group	−3.72 to −3.80
IOK	Inferior olive, cap of Kooy of the medial nucleus	−4.68 to −5.08
IOM	Inferior olive, medial nucleus	−2.80 to −3.80
IOPr	Inferior olive, principal nucleus	−2.80 to −4.30
IOVL	Inferior olive, ventrolateral protrusion	−4.24 to −4.30
IPA	Interpeduncular nucleus, apical subnucleus	2.28–1.96
IPC	Interpeduncular nucleus, caudal subnucleus	3.40–1.96
IPDL	Interpeduncular nucleus, dorsolateral subnucleus	2.96–2.70
IPDM	Interpeduncular nucleus, dorsomedial subnucleus	3.40–2.20
IPF	Interpeduncular fossa	3.80–3.70
IPi	Interpeduncular nucleus, intermediate subnucleus	2.96–1.96
IPl	Internal plexiform layer of the olfactory bulb	15.70–14.20
IPR	Interpeduncular nucleus, rostral subnucleus	3.40–2.70
IPRL	Interpeduncular nucleus, rostrolateral subnucleus	3.40–3.20
ipt	Interpedunculotegmental tract	1.96
Irt	Intermediate reticular nucleus	−1.30 to −4.30
jx	Juxtarestiform body	−1.80
K	Nucleus K	0.28–0.20
KF	Kolliker-fuse nucleus	0.28–0.20
La	Lateral amygdaloid nucleus	6.70–6.44
LA	Lateroanterior hypothalamic nucleus	7.70–7.60
lab	Longitudinal association bundle	6.44–6.20
LaDL	Lateral amygdaloid nucleus, dorsal part	7.20–4.84
Lat	Lateral (dentate) cerebellar nucleus	−1.52 to −2.60
LatC	Latreal cervical nucleus	C1–C5
LatPC	Lateral cerebellar nucleus, parvocellular part	−2.30 to −2.60
LaVL	Lateral amygdaloid nucleus, ventral part	6.20–5.40
LaVM	Lateral amygdaloid nucleus, ventromedial part	6.20–4.84
LC	Locus coeruleus	−0.16 to −1.52
Ld	Lambdoid septal zone	9.70–9.20
LDDM	Laterodorsal thalamic nucleus, dorsomedial part	6.88–5.70
LDTg	Laterodorsal tegmental nucleus	0.28 to −0.30
LDTgV	Laterodorsal tegmental nucleus, ventral part	0.28–0.20
LDVL	Laterodorsal thalamic nucleus, ventrolateral part	7.20–5.40
lfp	Longitudinal fasciculus of the pons	1.70–1.00
lfu	Lateral funiculus of the spinal cord	C1–C5

LH	Lateral hypothalamic area	7.70–4.48
LHb	Lateral habenular nucleus	6.88–6.20
LHbL	Lateral habenular nucleus, lateral part	5.86–4.84
LHbM	Lateral habenular nucleus, medial part	5.86–4.84
Li	Linear nucleus of the medulla	−3.30 to −3.72
ll	Lateral lemniscus	1.70–0.20
LLF	Lateral lemniscal fields	0.28
LM	Lateral mammillary nucleus	4.48–4.20
LMol	Lacunosonum moleculare layer of the hippocampus	5.20
lo	Lateral olfactory tract	15.20–7.60
LO	Lateral orbital cortex	14.20–11.20
LOT	Nucleus of the olfactory tract	8.08–7.20
LPB	Lateral parabrachial nucleus	0.28 to −0.80
LPBS	Lateral parabrachial nucleus, superior part	0.28–0.20
LPGi	Lateral paragigantocellular nucleus	−1.30 to −3.80
LPLC	Lateral posterior thalamic nucleus, laterocaudal part	4.48–3.70
LPLC	Lateral posterior thalamic nucleus, laterocaudal part	4.48–3.70
LPLR	Lateral posterior thalamic nucleus, laterorostral part	5.20–4.48
LPMC	Lateral posterior thalamic nucleus, mediocaudal part	4.48–3.20
LPMR	Lateral posterior thalamic nucleus, mediorostral part	6.20–4.48
LPO	Lateral preoptic area	8.74–8.08
LR4V	Lateral recess of the 4th ventricle	−0.30 to −3.30
LRt	Lateral reticular nucleus	−4.24 to −5.60
LRtPC	Lateral reticular nucleus, parvocellular part	−4.24 to −5.60
LRtS5	Lateral reticular nucleus, subtrigeminal part	−4.24 to −4.30
LSD	Lateral septal nucleus, dorsal part	10.20–8.08
LSI	Lateral septal nucleus, intermediate part	10.70–8.60
Lso	Lateral superior olive	0.20 to −1.04
LSV	Lateral septal nucleus, ventral part	10.70–8.60
LT	Lateral terminal nucleus of the accessory optic tract	3.80–3.40
ltg	Lateral tegmental tract	2.70–1.70
LV	Lateral ventricle	11.20–4.48
Lve	Lateral vestibular nucleus	−1.30 to −2.30
LVPO	Lateroventral periolivary nucleus	0.28 to −1.04
lvs	Lateral vestibulospinal tract	−1.80
m5	Motor root of the trigeminal nerve	2.28 to −0.80
MA3	Medial accessory oculomotor nucleus	3.70–3.20
mch	Medial corticohypothalamic tract	8.20–8.08
MCLH	Magnocellular nucleus of the lateral hypothalamus	6.20–5.70
mcp	Middle cerebellar peduncle	1.70 to −1.04
MCPC	Magnocellular nucleus of the posterior commissure	4.20–3.70
MCPO	Magnocellular preoptic nucleus	8.74–7.20
MD	Mediodorsal thalamic nucleus	7.20–5.40
MDC	Mediodorsal thalamic nucleus, central part	6.70–5.70
MdD	Medullary reticular nucleus, dorsal part	−4.68 to −5.60
MDL	Mediodorsal thalamic nucleus, lateral part	6.88–5.40
MDM	Mediodorsal thalamic nucleus, medial part	6.70–5.70
MDPL	Medodorsal thalamic nucleus, paralaminar part	6.44
MdV	Medullary reticular nucleus, ventral part	−4.68 to −5.60
Me	Medial amygdaloid nucleus	6.44–6.20
ME	Median eminence	6.88–5.70
Me5	Mesencephalic trigeminal nucleus	2.28 to −1.04
me5	Mesencephalic trigeminal tract	2.28 to −1.04
MeAD	Medial amygdaloid nucleus, anterodorsal part	6.88–6.70
MeAV	Medial amygdaloid nucleus, anteroventral part	6.88–6.70
Med	Medial (fastigial) cerebellar nucleus	−2.30 to −2.80

MedDL	Medial cerebellar nucleus, dorsolateral protuberance	−2.60
MePD	Medial amygdaloid nucleus, posterodorsal part	6.44–5.70
MePV	Medial amygdaloid nucleus, posteroventral part	6.20–5.40
mfb	Medial forebrain bundle	8.08–4.20
mfba	Medial forebrain bundle, ‘a’ component	11.70–8.20
mfbb	Medial forebrain bundle, ‘b’ component	9.70–8.20
MG	Medial geniculate nucleus	2.28–2.20
MGD	Medial geniculate nucleus, dorsal part	4.20–2.70
MGM	Medial geniculate nucleus, medial part	4.20–2.70
MGV	Medial geniculate nucleus, ventral part	4.20–2.70
MHb	Medial habenular nucleus	7.20–4.70
Mi	Mitral cell layer of the olfactory bulb	15.70–14.20
MiA	Mitral cell layer of the accessory olfactory bulb	14.70
Min	Minimus nucleus	3.40
MiTg	Microcellular tegmental nucleus	1.96–1.00
ML	Medial mammillary nucleus, lateral part	4.48–4.20
ml	Medial lemniscus	5.86–4.30
ML	Medial mammillary nucleus, lateral part	4.48–4.20
mlf	Medial longitudinal fasciculus	3.40 to −5.60
MM	Medial mammillary nucleus, medial part	4.70–4.20
MMn	Medial mammillary nucleus, median part	4.70–4.48
MnA	Median accessory nucleus of the medulla	−5.60
MnPO	Median preoptic nucleus	8.74–8.60
MnR	Medial raphe nucleus	1.70–0.70
MO	Medial orbital cortex	14.20–12.70
Mo5	Motor trigeminal nucleus	0.20 to −0.80
Mol	Molecular layer of the dentate gyrus	5.20
MP	Medial mammillary nucleus, posterior part	4.20–3.40
mp	Mammillary peduncle	4.48–3.20
MPA	Medial preoptic area	8.74–7.60
MPB	Medial parabrachial nucleus	0.28 to −1.04
MPO	Medial preoptic nucleus	8.20–8.08
MPOC	Medial preoptic nucleus, central part	8.20–8.08
MPT	Medial pretectal nucleus	3.70
MRe	Mammillary recess of the 3rd ventricle	4.84–4.48
MS	Medial septal nucleus	10.20–8.74
MSO	Medial superior olive	0.28 to −1.04
mt	Mammillothalamic tract	7.20–4.20
MT	Medial terminal nucleus of the accessory optic tract	3.80–3.70
mtg	Mammillotegmental tract	4.70–3.70
MTu	Medial tuberal nucleus	5.86–5.40
MVe	Medial vestibular nucleus	−1.30 to −3.80
MVeV	Medial vestibular nucleus, ventral part	−1.52 to −2.96
MVPO	Medioventral periolivary nucleus	0.28 to −1.04
MZMG	Marginal zone of the medial geniculate	3.80–2.96
O	Nucleus O	−0.68 to −0.80
Obex	Obex	−5.30
OBl	Outer blade of the dentalte gyrus	4.84–4.70
oc	Olivocerebellar tract	−3.72 to −4.30
OC1B	Occipital cortex area 1, binocular part	3.20 to −0.30
OC1M	Occipital cortex area 1, monocular part	3.20 to −0.30
Oc2L	Occipital cortex area 2, lateral part	5.20 to −0.30
Oc2L	Occipital cortex area 2, lateral part	5.20 to −0.30
Oc2ML	Occipital cortex area 2, mediolateral part	5.20–2.20
Oc2ML	Occipital cortex area 2, mediolateral part	5.20–2.20
Oc2MM	Occipital cortex area 2, mediomedial part	5.20–0.70

Oc2MM	Occipital cortex area 2, mediomedial part	5.20–0.70
Ocb	Olivocochlear bundle	−0.68 to −1.30
ON	Olfactory nerve layer	15.70–14.70
Op	Optic nerve layer of the superior colliculus	3.40–1.00
opt	Optic tract	7.20–3.70
OPT	Olivary pretectal nucleus	4.48–3.70
Or	Oriens layer of the hippocampus	5.20
OT	Nucleus of the optic tract	3.80–2.96
OV	Olfactory ventricle	15.70–11.70
ox	Optic chiasma	7.20–3.70
P5	Peritrigeminal zone	0.28 to −0.80
P7	Perifacial zone	−1.30 to −2.60
Pa4	Paratrochlear	1.70–1.36
Pa5	Paratrigeminal nucleus	−3.72 to −4.30
Pa6	Paraabducens nucleus	−1.04 to −1.30
PaAP	Paraventricular hypothalamic nucleus, anterior parvocellular part	7.70–7.60
PaDC	Paraventricular hypothalamic nucleus, dorsomedial cap	7.20
PaLM	Paraventricular hypothalamic nucleus, lateral magnocellular part	7.20
PaMP	Paraventricular hypothalamic nucleus, parvocellular part	7.20–6.88
PaPo	Paraventricular hypothalamic nucleus, posterior part	6.88–6.70
Par 1	Pariental cortex, area 1	11.70–3.70
Par 2	Pariental cortex, area 2	9.20–5.70
PaV	Paraventricular hypothalamic nucleus, ventral part	7.20
PBG	Parabigeminal nucleus	1.96–1.00
PC	Paracentral thalamic nucleus	7.70–5.40
pc	Posterior commissure	4.20–3.70
PCF	Precommisural fissure	−1.04 to −2.30
PCGS	Paracochlear glial substance	−0.68 to −1.04
PCom	Nucleus of the posterior commissure	3.80–3.70
PCRt	Parvocellular reticularis nucleus	−2.60 to −4.30
PCRtA	Parvocellular reticularis nucleus, alpha part	−1.04 to −2.30
PCTg	Paracollicular tegmentum	−0.30 to −0.68
pd	Predorsal bundle	−0.68 to −3.30
PDR	Paradorsal raphe nucleus	1.00
PDTg	Posterodorsal tegmental nucleus	−0.68 to −1.04
Pe	Periventricular hypothalamic nucleus	8.74 to −6.20
PeF	Perifornical nucleus	6.20–5.40
PF	Parafascicular thalamic nucleus	5.20–4.48
PFl	Paraflocculus	−0.20 to −2.96
PH	Posterior hypothalamic area	5.40–4.70
Pi	Pineal gland	0.70
PIL	Posterior intralaminar thalamic nucleus	4.20–2.96
Pir	Piriform cortex	12.70–4.48
PiRe	Pineal recess	4.48–3.20
PL	Paralemniscal nucleus	1.70–0.70
PLCo	Posterolateral cortical amygdaloid nucleus (C2)	6.70–4.48
PLd	Paralambdoid septal nucleus	9.20
PLF	Posterolateral fissure	−0.68 to −1.30
PLi	Posterior limitans thalamic nucleus	4.20–3.20
Pli	Posterior limitans thalamic nucleus	4.20–3.20
PM	Paramedian lobule	−3.30 to −5.30
PMCo	Posteromedial cortical amygdaloid nucleus	5.86–2.96
PMD	Premammillary nucleus, dorsal part	4.84–4.70
PMn	Paramedian reticularis nucleus	−3.72 to −4.80
PMR	Paramedian raphe nucleus	1.36–0.17
PMV	Premammillary nucleus, ventral part	5.20–4.84

PN	Paranigral nucleus	3.80–3.20
Pn	Pontine nuclei	2.28–1.00
PnC	Pontine reticular nucleus, caudal part	−0.16 to −1.30
PnO	Pontine reticular nucleus, oral part	1.70–0.20
PnV	Pontine reticular nucleus, ventral part	−0.16 to −1.04
Po	Posterior thalamic nuclear group	6.44–4.48
PoDG	Polymorph layer of the dentate gyrus	6.44–2.70
PoMn	Posteromedian thalamic nuclear	5.20
PoT	Posterior thalamic nuclear group, triangular part	4.48–3.20
POT	Posterior thalamic nuclear group, triangular part	4.48–3.20
PP	Parapeduncular nucleus	4.20–2.96
PPF	Prepyramidal fissure	−3.72 to −5.08
PPT	Posterior pretectal nucleus	3.80–3.20
PPTg	Pedunculopontine tegmental nucleus	2.28–0.70
PR	Prerubral field	4.84–3.80
Pr5	Principal sensory trigeminal nucleus	0.28
Pr5DM	Principal sensory trigeminal nucleus, dorsomedial part	−0.30 to −1.04
Pr5VL	Principal sensory trigeminal nucleus, ventrolateral part	0.20 to −1.04
prb	Probst’s bundle	−1.04 to −4.68
Prb	Nucleus of the Probst’s bundle	−4.24 to −4.68
PrC	Precommissural nucleus	4.70–4.48
PRh	Perirhinal cortex	7.20 to −0.30
Pr	Prepositus nucleus	−1.80 to −3.30
PS	Parastrial nucleus	8.74–8.60
PSF	Posterior superior fissure	−0.80 to −2.00
Psol	Parasolitary nucleus	−4.24 to −4.68
PT	Paratenial thalamic nucleus	8.08–7.20
PV	Paraventricular thalamic nucleus	6.70–6.20
pv	Periventricular fiber system	4.84–4.48
PVA	Paraventricular thalamic nucleus, anterior part	8.08–6.88-1
PVP	Paraventricular thalamic nucleus, posterior part	5.86–4.48
Py	Pyramidal cell layer of the hippocampus	5.20
py	Pyramidal tract	0.70 to −5.08
pyx	Pyramidal decussation	−5.30 to −5.60
R	Red nucleus	3.20
Rad	Stratum of the hippocampus	5.20
Ramb	Retroambiguus nucleus	−5.08 to −5.60
Rbd	Rhabdoid nucleus	2.20–0.70
RCh	Retrochiasmatic area	7.20
Re	Reuniens thalamic nucleus	7.70–5.70
ReIC	Recess of the inferior colliculus	0.28 to −0.30
Reth	Retroethmoid nucleus	3.80–3.70
RF	Rhinal fissure	14.20–1.00
Rh	Rhomboid thalamic nucleus	7.70–5.70
RI	Rostral interstitial nucleus of the medial longitudinal fasciculus	4.70–4.20
RL	Retrolemniscal nucleus	−0.16
Rli	Rostral linear nucleus of the raphe	3.80–3.20
RMC	Red nucleus, magnocellular part	3.40–2.70
RMg	Raphe magnus nucleus	−0.16 to −2.60
Ro	Nucleus of Roller	−3.72 to −4.80
Rob	Raphe obscurus nucleus	−2.60 to −5.30
Rpa	Raphe pallidus (postpyramidal raphe) nucleus	−0.80 to −5.08
RpC	Red nucleus, parvocellular part	3.70–2.70
RPn	Raphe pontis nucleus	0.28 to −0.30
RPO	Rostral periolivary region	1.00–0.28
RR	Retrorubral nucleus	1.96–1.36

RRF	Retrorubral field	2.28–1.96
rs	Rubrospinal tract	2.28 to −2.30
RSA	Retrosplenial agranular cortex	7.20 to −0.30
RSG	Retrosplenial granular cortex	7.20–1.20
Rt	Reticular thalamic nucleus	7.70–4.84
RtTg	Reticulotegmental nucleus of the pons	1.36–0.70
RtTgP	Reticulotegmental nucleus of the pons, pericentral part	1.36–0.70
RVL	Rostroventrolateral reticular nucleus	−2.30 to −5.08
s5	Sensory root of the trigeminal nerve	2.70 to −0.80
sag	Sagulum nucleus	0.70 to −0.16
Sc	Scaphoid thalamic nucleus	4.48
SC	Superior colliculus	3.70
scc	Splenium of the corpus callosum	4.20–3.70
SCh	Suprachiasmatic nucleus	8.08–7.60
SCO	Subcommissural organ	4.20
scp	Superior cerebellar peduncle	6.44 to −2.00
SF	Secondary fissure	−3.72 to −5.30
SFi	Septofimbrial nucleus	8.74–8.08
SFO	Subfornical organ	8.20–7.60
SG	Suprageniculate thalamic nucleus	4.20–2.70
Sge	Supragenual nucleus	−1.30 to −1.52
SHi	Septohippocampal nucleus	10.70–9.20
SHy	Septohypothalamic nucleus	8.74–8.60
SI	Substantia innominata	8.74–6.88
Sim	Simple lobule	−0.30 to −2.60
SM	Nucleus of the stria medullaris	7.70–7.60
sm	Stria medullaris of the thalamus	8.20–4.84
SMT	Submammillothalamic nucleus	4.84–4.70
SNC	Substantia nigra, compact part	4.20–2.70
SNL	Substantia nigra, lateral part	3.80–2.96
SNR	Substantia nigra, reticular part	4.48–2.70
So	Supraoptic nucleus	8.20–7.20
Sol	Nucleus of the solitary tract	−1.52 to −5.60
sol	Solitary tract	−2.60 to −5.60
SolC	Nucleus of the solitary tract, commissural tract	−4.68 to −5.60
SolG	Nucleus of the solitary tract, gelatinous tract	−4.30
SolL	Nucleus of the solitary tract, lateral part	−2.96 to −4.30
SolM	Nucleus of the solitary tract, medial part	−2.96 to −4.30
SOR	Supraoptic nucleus, retrochiasmatic (diffuse) part	6.88–5.86
sox	Supraoptic decussation	7.20–4.48
sp5	Spinal trigeminal tract	−1.04 to −5.60
Sp5C	Spinal trigeminal nucleus, caudal part	−4.68 to −5.60
Sp5I	Spinal trigeminal nucleus, interpolar part	−2.80 to −4.80
Sp5O	Spinal trigeminal nucleus, oral part	−1.04 to −2.60
SPF	Subparafascicular thalamic nucleus	5.20–4.84
SPFPC	Subparafascicular thalamic nucleus, parvocellular part	4.70–4.20
SPFPC	Subparafascicular thalamic nucleus, parvocellular part	4.70–4.20
Sph	Sphenoid nucleus	−0.68 to −0.80
SPO	Superoir paraolivary nucleus	0.28 to −1.04
SPTg	Subpeduncular tegmental nucleus	1.36–0.70
SpVe	Spinal vestibular nucleus	−2.00 to −3.30
SStr	Substriatal area	8.08–7.60
st	Stria terminalis	8.74–5.20
StA	Strial part of the preoptic area	8.74–8.60
Stg	Stigmoid hypothalamic nucleus	6.88–6.70
STh	Subthalamic nucleus	5.40–4.70

StHy	Striohypothalamic nucleus	8.20–8.08
str	Superior thalamic nucleus	4.84–4.20
Su3	Supraoculomotor central gray	2.96–1.96
Su5	Supratrigeminal nucleus	0.20 to −0.30
SubB	Subbrachial nucleus	2.28–1.70
SubCA	Subcoeruleus nucleus, alpha part	−0.16 to −0.80
SubCD	Subcoeruleus nucleus, dorsal part	0.28 to −0.80
SubCV	Subcoeruleus nucleus, ventral part	0.28 to −0.80
SubG	Subgeniculate nucleus	4.84–4.48
SubI	Subincertal nucleus	6.20–5.40
SuG	Superficial gray layer of the superior colliculus	3.40–1.00
SuM	Supramammillary nucleus	4.84–4.20
sumx	Supramammillary decussation	4.70–4.20
SuS	Superior salivatory nucleus	−1.52
SuVe	Superior vestibular nucleus	−1.04 to −2.00
TC	Tuber cinereum area	7.20–5.70
Te	Terete hypothalamic nucleus	5.70–4.84
Te1	Temporal cortex area 1	5.20–2.70
Te2	Temporal cortex, area 2	2.20–0.70
Te3	Temporal cortex, area 3	5.20–2.70
tfp	Transverse fibers of the pons	2.70–1.00
TM	Tuberomammillary nucleus	5.20–4.70
TMC	Tuberal magnocellular nucleus	5.20–4.84
TS	Triangular septal nucleus	8.20–7.20
ts	Tectospinal tract	2.28–0.20
TT	Tenia tecta	13.20–2.70
Tu	Olfactory tubercle	12.20–8.20
TuPl	Olfactory tubercle, plexiform layer	11.70
TuPo	Olfactory tubercle, polymorph layer	11.70
TuPy	Olfactory tubercle, pyramidal layer	11.70
TZ	Nucleus of the trapezoid body	0.70 to −1.04
tz	Trapezoid body	0.70–1.80
unc	Unicate fasciculus	−1.04 to −1.52
vaf	Ventral amygdalofugal pathway	6.88
VCA	Ventral cochlear nucleus, anterior part	0.20 to −1.30
VCP	Ventral cochlear nucleus, posterior part	−1.52 to −2.30
VDB	Nucleus of the vertical limb of the diagonal blend	10.20–9.20
VEn	Ventral endopiriform nucleus	9.20–5.40
vfu	Ventral funiculus of the spinal cord	C1–C5
vhc	Ventral hippocampal commisure	8.20–7.60
VL	Ventrolateral thalamic nucleus	7.20–5.86
VLGMC	Ventral lateral geniculate nucleus, magnocellular part	4.84–4.20
VLGPC	Ventral lateral geniculate nucleus, parvocellular part	4.84–4.20
VLL	Ventral nucleus of the lateral lemniscus	1.36–0.70
VLO	Ventrolateral orbital cortex	13.20–11.20
VLPB	Ventrolateral parabrachial nucleus	−0.16
VLTg	Ventrolateral tegmental area	1.00–0.70
VM	Ventromedial thalamic nucleus	7.20–5.40
VMH	Ventromedial hypothalamic nucleus	6.88–5.40
VMHC	Ventromedial hypothalamic nucleus, central part	5.86–5.70
VMHDM	Ventromedial hypothalamic nucleus, dorsomedial part	5.86–5.70
VMHVL	Ventromedial hypothalamic nucleus, ventrolateral part	5.86–5.70
VmnF	Ventralmedian fissure of the spinal cord	C1–C5
VN	Vomeronasal nerve layer	15.20–14.70
VO	Ventral orbital cortex	14.20–12.70
VP	Ventral pallidum	11.20–8.08

VPL	Ventral posterolateral thalamic nucleus	6.88–4.84
VPM	Ventral posteromedial thalamic nucleus	6.70–4.70
vr	Ventral root of spinal nerve	C1–C5
vsc	Ventral spinocerebellar tract	0.28 to −1.04
VTA	Ventral tegmental area (Tsai)	4.20–2.20
VTg	Ventral tegmental nucleus (Gudda)	0.70–0.20
vtgx	Ventral tegmental decussation	2.28–2.20
VTRZ	Visual tegmental relay zone	3.80–3.40
X	Nucleus X	−2.00 to −3.80
xcsp	Decussation of the superior cerebellar peduncle	1.96–1.00
Xi	Xiphoid thalamic nucleus	6.88–6.70
Y	Nucleus Y	−2.00 to −2.30
Z	Nucleus Z	−4.24
ZI	Zona incerta	7.20–4.20
ZID	Zona incerta, dorsal part	5.40–4.48
ZIV	Zona incerta, ventral part	5.40–4.48
ZL	Zona limitans	9.70
Zo	Zonal layer of the superior colliculus	3.40–1.00

Acknowledgments

We thank Ms. Marian Adly for her excellent preparation of the manuscript.

References

[1] Bauer FE, Adrian TE, Yanaihara N, Polak LM, Bloom SR. Chromatographic evidence for high molecular mass galanin immunoreactivity in pig and cat adrenal glands. FEBS Lett 1986;201: 327–31.
[2] Bauer FE, Venetikou M, Burrin JM, Ginsberg L, Mackay DJ, Bloom SR. Growth hormone release in man induced by galanin, a new hypothalamic peptide. Lancet 1986;2:192–4.
[3] Cella SG, Locatelli V, De Gennaro V, Bondiolotti GP, Pintor C, Loche S, et al. Epinephrine mediates the growth hormone-releasing effect of galanin in infant rats. Endocrinology 1988;122:855–9.
[4] Chan-Palay V. Galanin hyperinnervates surviving neurons of the human basal nucleus of Meynert in demnetias of Alzheimer's and Parkinson's disease: a hypothesis for the role of galanin in accentuating cholinergic dysfunction in dementia. J Comp Neurol 1988;273:543–57.
[5] Chatterjee VK, Ball IA, Proby C, Burrin IM, Bloom SR. Galanin abolishes the inhibitory effect of cholinergic blockade on growth hormone-releasing hormone-induced secretion of growth hormone in man. J Endocrinol 1988;116:R1–2.
[6] Ch'ng ILC, Christofides ND, Anand P, Gibson I, Allen YS, Su HC, et al. Distribution of galanin immunoreactivity in the central nervous system and the responses of galanin-containing neuronal pathways to injury. Neuroscience 1985;16:343–54.
[7] Clarke PBS, Hamill GS, Nadi NS, Jacobowitz DM, Pert A. ^{3}H-nicotine and ^{125}I-alpha bungarotoxin labeled nicotinic receptors in the interpeduncular nucleus of rats. II. Effects of habenular deafferentation. J Comp Neurol 1986;251:407–13.
[8] Coons AH. Fluorescence antibody methods. In: Danielli IF, editor. General cytochemical methods. New York: Academic Press; 1958. p. 399–422.
[9] Counts SE, Perez SE, Kahl U, Bartfai T, Bowser RP, Deecher DC, et al. Galanin: neurobiologic mechanisms and therapeutic potential for Alzheimer's disease. CNS Drug Rev 2001;7:445–70.
[10] Crawley JN, Muson EJ, Hohmann JG, Teklemichael D, Steiner RA, Holmberg K, et al. Galanin overexpressing transgenic mice. Neuropeptides 2002;36:145–56.
[11] Dahlström A, Fuxe K. Evidence for the existence of monoamine neurons in the central nervous system. Demonstration of monoamines in the cell bodies of brain stem neurons. Acta Physiol Scand 1964;62(Suppl):1–55.
[12] Diz DI, Jacobowitz DM. Cardiovascular actions of four neuropeptides in the rat hypothalamus. Clin Exp Hypertens 1984;6:2085–90.
[13] Diz DI, Jacobowitz DM. Cardiovascular effects of discrete intrahypothalamic and preoptic injections of bradykinin. Brain Res Bull 1984;12:409–17.
[14] Diz DI, Jacobowitz DM. Cardiovascular effects of intrahypothalamic injection of α-melanocyte stimulating hormone. Brain Res 1983;270:265–72.
[15] Diz DI, Jacobowitz DM. Cardiovascular effects produced by injection of thyrotropin-releasing hormone in specific preoptic and hypothalamic nuclei in the rat. Peptides 1984;5:801–8.
[16] Diz DI, Vitale JA, Jacobowitz DM. Increases in heart rate and blood pressure produced by injections of dermorphin into discrete hypothalamic sites. Brain Res 1984;294:47–57.
[17] Everett BI, Meister B, Hökfelt T, Melander T, Terenius L, Rökaeus A, et al. The hypothalamic arcuate nucleus–median eminence complex: immunohistochemistry of transmitters, peptides and DARPP-32 with special reference to coexistence in dopamine neurons. Brain Res 1986;396:97–155.
[18] Fisone G, Wu CF, Consolo S, Brynne N, Bartfai T, Melander T, et al. Galanin inhibits acetylcholine release in the ventral hippocampus of the rat: histochemical, autoradiographic, in vivo, and in vitro studies. Proc Natl Acad Sci USA 1987;88:7339–43.
[19] Gibson SI, McCrossan MV, Polak IM. A subset of calcitonin gene-related peptide (CGRP)-immunoreactive cells contain substance P (SP), somatostatin (SOM) or galanin (GAL) immunoreactivity in pig dorsal root ganglia. Regul Pept 1985;13:68.
[20] Goodfriend TL, Levin L, Fasman GD. Antibodies to bradykinin and angiotensin: the use of carbodiimide in immunology. Science NY 1969;144:1344–6.
[21] Harro J, Oreland L. Depression as a spreading adjustment disorder of monoaminergic neurons: a case for primary implication of the locus coeruleus. Brain Res Brain Res Rev 2001;38:79–128.
[22] Herkenham M. Mismatches between neurotransmitter and receptor localizations in brain: observations and implications. Neuroscience 1987;23:1–38.

[23] Hökfelt T, Barfai T, Jacobowitz DM, Ottoson D, editors. Galanin: a new multifunctional peptide in the neuro-endocrine system. Cambridge, UK: MacMillan Press; 1991.
[24] Hökfelt T, Johansson O, Goldstein M. Central catecholamine neurons as revealed by immunohistochemistry with special reference to adrenaline neurons. In: BjörkJund A, Hökfelt T, editors. Handbook of chemical neuroanatomy, Vol. 2. Classical transmitters in the CNS, Part I. Amsterdam: Elsevier; 1984. p. 157–276.
[25] Hökfelt T, Martensson R, BjörkJund A, Kleinau S, Goldstein M. Distribution maps of tyrosine-hydroxylase-immunoreactive neurons in the rat brain. In: BjörkJund A, Hökfelt T, editors. Handbook of chemical neuroanatomy, Vol. 2. Classical transmitters in the CNS, Part I. Amsterdam: Elsevier; 1984. p. 277–379.
[26] Holmes A, Kinney JW, Wrenn CC, Li Q, Yang RJ, Ma L, et al. Galanin GAL-R1 receptor null mutant mice display increased anxiety-like behavior specific to the elevated plus-maze. Neuropsychopharmacology 2003;28:1031–44.
[27] Ichikawa H, Deguchi T, Nakago T, Jacobowitz DM, Sugimoto T. Parvalbumin, calretinin and carbonic anhydrase in the trigeminal and spinal primary neurons of the rat. Brain Res 1994;655:241–5.
[28] Jacobowitz DM. Histochemical and micropunch analysis of aminergic and cholinergic pathways. In: Deniker P, RadoncoThomas C, Villeneuve N, editors. Collegium internationale neuropsychopharmacologicum. 10th International Congress, Quebec; 1978.
[29] Jacobowitz DM. Monoaminergic pathways in the central nervous system. In: Lipton MA, DiMascio A, Killam KF, editors. Psychopharmacology: a generation of progress. New York: Raven Press; 1978. p. 119–30.
[30] Jacobowitz DM. Removal of discrete fresh regions of the rat brain. Brain Res 1974;80:111–5.
[31] Jacobowitz DM, Abbott LC. Chemoarchitectonic atlas of the developing mouse brain. Boca Raton: CRC Press; 1998.
[32] Jacobowitz DM, Creed GJ. Cholinergic projection sites of the nucleus of tractus diagonalis. Brain Res Bull 1983;10:365–71.
[33] Jacobowitz DM, MacLean PD. A brainstem atlas of catecholaminergic neurons and serotonergic perikarya in a pygmy primate (cebuella pygmaea). J Comp Neurol 1978;177:397–415.
[34] Jacobowitz DM, O'Donohue TL. α-MSH: immunohistochemical identification and mapping in neurons of the rat brain. Proc Natl Acad Sci USA 1978;75:6300–4.
[35] Jacobowitz DM, O'Donohue TL, Chey WY, Chang TM. Mapping of motilin-immunoreactive neurons of the rat brain. Peptides 1981;2:479–87.
[36] Jacobowitz DM, Palkovits M. Topographic atlas of catecholamine and acetylcholinesterase containing neurons in the brain. Forebrain (Telencephalon, Diencephalon). J Comp Neurol 1974;157:13–28.
[37] Jacobowitz DM, Roizen MF, Suttora NL, Muth EA. A method for the discrete removal of a segment of the dorsal noradrenergic bundle and its application to analysis of catecholamine and dopamine-beta-hydroxylase. Brain Res 1975;98:377–82.
[38] Jacobowitz DM, Schulte H, Chrousos GP, Loriaux DM. Localization of GRF-like immunoreactive neurons in the rat brain. Peptides 1983;4:521–4.
[39] Jacobowitz DM, Skofitsch G, Eskay RL, Keiser HR, Zamir N. Evidence for the existence of atrial natriuretic factor-containing neurons in the rat brain. Neuroendocrinology 1985;40:92–4.
[40] Ju G, Hökfelt T, Brodin E, Fahrenkrug J, Fischer JA, Frey P, et al. Primary sensory neurons of the rat showing calcitonin gene-related peptide-immunoreactive, somatostatin-immunoreactive, galanin-immunoreactive, vasoactive intestinal polypeptide-immunoreactive and cholecystokinin-immunoreactive ganglion cells. Cell Tiss Res 1987;247:417–31.
[41] Ju G, Melander T, Ceccatelli S, Hökfelt T, Frey P. Immunohistochemical evidence for a spinothalamic pathway co-containing cholecystokinin and galanin-like immunoreactivities in the rat. Neuroscience 1987;20:439–56.
[42] Klotzenburg M, Gibson S, Fitzgerald M, Bloom SR, Polak JM. Postnatal development of calcitonin gene-related peptide (CGRP)-like, substance P (SP)-like, galanin (GAL)-like and thyrotropin releasing hormone (TRH)-like immunoreactivity in the rat lumbar spinal cord. Regul Pept 1984;9:337.
[43] Köhler C, Ericson H, Watanabe T, Polak JM, Palay SL, Palay V, et al. Galanin immunoreactivity in hypothalamic histamine neurons: further evidence for multiple chemical messengers in the tuberomamillary nucleus. J Comp Neurol 1986;250:58–64.
[44] König JFR, Klippel RA. The rat brain. A stereotaxic atlas. New York: Krieger Publishing; 1963.
[45] Koshiyma H, Kato Y, Inoue T, Murakami Y, Ishikawa Y, Yanaihara N, et al. Central galanin stimulates pituitary prolactin secretion in rats: possible involvement of hypothalamic vasoactive intestinal polypeptide. Neurosci Lett 1987;75:49–54.
[46] Kyrkouli SE, Stanley BG, Leibowitz SF. Galanin: stimulation of feeding induced by medial hypothalamic injection of this novel peptide. Eur J Pharmacol 1986;122:159–60.
[47] Leibowitz SF. Brain neurotransmitters and appetite regulation. Psychopharmacol Bull 1985;21:412–30.
[48] Leibowitz SF. Hypothalamic neuropeptide Y, galanin, and amines. Concepts of coexistence in relation to feeding behavior. Ann NY Acad Sci 1989;575:221–33.
[49] Levin MC, Sawchenko PE, Howe PR, Bloom SR, Polak JM. Organization of galanin-immunoreactive inputs to the paraventricular nucleus with special reference to their relationship to catecholaminergic afferents. J Comp Neurol 1987;261:562–82.
[50] Liu HX, Hökfelt T. The participation of galanin in pain processing at the spinal level. Trends Pharmacol Sci 2002;23:468–74.
[51] Marti E, Gibson SI, Facer P, Krotzenburg M, Polak IM. Neuronal maturation in human and rat spinal cord assessed by immunoreactivity for substance P, calcitonin gene-related peptide (CGRP), galanin and neurofilament proteins. Regul Pept 1985;13:65.
[52] Marti E, Gibson SI, Polak IM, Facer P, Springall DR, Van Aswegen G, et al. Ontogeny of peptide- and amine-containing neurones in motor, sensory, and autonomic regions of rat and human spinal cord, dorsal root ganglia, and rat skin. J Comp Neurol 1987;266:332–59.
[53] Massari VJ, Tizabi Y, Jacobowitz DM. Potential noradrenergic regulation of serotonergic neurons in the median raphe nucleus. Exp Brain Res 1979;34:177–82.
[54] Mazarati AM, Halaszi E, Telegdy G. Anticonvulsive effects of galanin administered into the central nervous system upon the picrotoxin-kindled seizure syndrome in rats. Brain Res 1992;589:164–6.
[55] Mazarati AM, Hohmann JG, Bacon A, Liu H, Sankar R, Steiner RA, et al. Modulation of hippocampal excitability and seizures by galanin. J Neurosci 2000;20:6276–81.
[56] Mazarati AM, Liu H, Soomets U, Sankar R, Shin D, Katsumori H, et al. Galanin modulation of seizures and seizure modulation of hippocampal galanin in animal models of status epilepticus. J Neurosci 1998;18:10070–7.
[57] Melander T, Fuxe K, Härfstrand A, Eneroth P, Hökfelt T. Effects of intraventricular injections of galanin on neuroendocrine functions in the male rat. Possible involvement of hypothalamic catecholamine neuronal systems. Acta Physiol Scand 1987;131:25–32.
[58] Melander I, Hökfelt T, Nilsson S, Brodin E. Visualization of galanin binding sites in the rat central nervous system. Eur J Pharmacol 1986;124:381–2.
[59] Melander T, Hökfelt T, Rökaeus A. Distribution of galanin-like immunoreactivity in the rat central nervous system. J Comp Neurol 1986;248:475–517.
[60] Melander T, Hökfelt T, Rökaeus A, Cuello AC, Oertel WH, Verhofstad A, et al. Coexistence of galanin-like immunoreactivity with catecholamines, 5-hydroxytryptamine, GABA and neuropeptides in the rat CNS. J Neurosci 1986;6:3640–54.

[61] Melander T, Staines WA. A galanin-like peptide coexists in putative cholinergic somata of the septum–basal forebrain complex and in acetylcholinesterase containing fibers and varicosities within the hippocampus of the owl monkey (*Aotus trivirgatus*). Neurosci Lett 1986;68:17–22.

[62] Melander T, Staines W, Hökfelt T, Rökaeus A, Eckstein F, Salvaterra PM, et al. Galanin-like immunoreactivity in cholinergic neurons of the septum–basal forebrain complex projecting to the hippocampus of the rat. Brain Res 1985;360:130–8.

[63] Melander T, Staines WA, Rökaeus A. Galanin-like immunoreactivity in hippocampal afferents in the rat with special reference to cholinergic and noradrenergic inputs. Neuroscience 1986;19:223–40.

[64] Mesulam MM, Mufson EI, Wainer BH, Levey AI. Central cholinergic pathways in the rat: an overview based on an alternative nomenclature (Ch1–Ch6). Neuroscience 1983;10:1185–201.

[65] Murakami Y, Kato Y, Koshiyama H, Inoue T, Yanaihara N, Imura H. Galanin stimulates growth hormone (GH) secretion via GH-releasing factor (GRF) in conscious rats. Eur J Pharmacol 1987;136:415–8.

[66] Nguyen KQ, Sills MA, Jacobowitz DM. Cardiovascular effects produced by microinjection of calcitonin gene-related peptide into the rat central amygdaloid nucleus. Peptides 1986;7:337–9.

[67] O'Donohue TL, Crowley WR, Jacobowitz DM. Biochemical mapping of the noradrenergic ventral bundle projection sites: evidence for a noradrenergic–dopaminergic interaction. Brain Res 1979;172:87–100.

[68] Olschowka JA, O'Donohue TL, Jacobowitz DM. The distribution of bovine pancreatic polypeptide-like immunoreactive neurons in rat brain. Peptides 1981;2:309–31.

[69] Olschowka JA, O'Donohue TL, Mueller GP, Jacobowitz DM. Hypothalamic and extrahypothalamic distribution of CRF-like immunoreactive neurons in the rat brain. Neuroendocrinology 1982;35:305–8.

[70] Olschowka JA, O'Donohue TL, Mueller GP, Jacobowitz DM. The distribution of corticotropin releasing factor-like immunoreactive neurons in rat brain. Peptides 1982;3:995–1015.

[71] Ottlecz A, Samson WK, McCann SM. Galanin: evidence for a hypothalamic site of action to release growth hormone. Peptides 1986;7:51–3.

[72] Palkovits M. Isolated removal of hypothalamic or other brain nuclei of the rat. Brain Res 1973;59:449–50.

[73] Palkovits M, Jacobowitz DM. Topographic atlas of catecholamine and acetylcholinesterase containing neurons in the brain. II. Hindbrain (Mesencephalon, Rhombencephalon). J Comp Neurol 1974;157:29–41.

[74] Palkovits M, Rökaeus A, Antoni FA, Kiss A. Galanin in the hypothalamo hypophyseal system. Neuroendocrinology 1987;46: 417–23.

[75] Paxinos G, Watson C. The rat brain in stereotaxic coordinates, 2nd ed. Sydney: Academic Press; 1986.

[76] Price IL. The efferent projections of the amygdaloid complex in the rat, cat and monkey. In: Ben-Ari Y, editor. The amygdaloid complex. INSERM Symposium No. 20. Amsterdam: Elsevier/North-Holland Biomedical Press; 1981. p. 121–32.

[77] Roizen MF, Jacobowitz DM. Studies on the origin of innervation of the noradrenergic areas bordering on the nucleus raphe dorsalis. Brain Res 1976;101:561–8.

[78] Rökaeus A, Young WS, Mezey E. Galanin coexists with vasopressin in the normal rat hypothalamus and galanin's synthesis is increased in the Brattleboro (diabetes insipidus) rats. Neurosci Lett 1988;90:45–50.

[79] Sahu A, Crowley WR, Tatemoto K, Balasubramaniam A, Kalra SP. Effects of neuropeptide Y on LH release in ovariectomized (ovx) and ovx estrogen, progesterone-treated rats. Peptides 1987;8:921–6.

[80] Sills MA, Nguyen KQ, Jacobowitz DM. Increases in the heart rate and blood pressure produced by microinjections of atrial natriuretic factor into the AV3V region of rat brain. Peptides 1985;6:1037–42.

[81] Skofitsch G, Jacobowitz DM. Atrial natriuretic peptide in the central nervous system of the rat. Cell Mol Neurobiol 1988;8:339–91.

[82] Skofitsch G, Jacobowitz DM. Autoradiographic distribution of ^{125}I calcitonin gene-related peptide binding sites in the rat central nervous system. Peptides 1985;6:975–86.

[83] Skofitsch G, Jacobowitz DM. Calcitonin gene-related peptide: detailed immunohistochemical distribution in the rat central nervous system. Peptides 1985;6:721–46.

[84] Skofitsch G, Jacobowitz DM. Calcitonin gene-related peptide coexists with substance P in capsaicin sensitive ganglia of the rat. Peptides 1985;6:747–54.

[85] Skofitsch G, Jacobowitz DM. Distribution of corticotropin releasing factor-like immunoreactivity in the rat brain by immunohistochemistry and radioimmunoassay: comparison and characterization of bovine and rat/human CRF antisera. Peptides 1985;6:319–36.

[86] Skofitsch G, Jacobowitz DM. Galanin-like immunoreactivity in capsaicin sensitive sensory neurons and ganglia. Brain Res Bull 1985;15:191–5.

[87] Skofitsch G, Jacobowitz DM. Quantitative distribution of galanin-like immunoreactivity in the rat central nervous system. Peptides 1986;7:609–13.

[88] Skofitsch G, Jacobowitz DM. Immunohistochemical mapping of galanin-like neurons in the rat central nervous system. Peptides 1985;6:509–46.

[89] Skofitsch G, Jacobowitz DM, Eskay RL, Zamir N. Distribution of atrial natriuretic factor-like immunoreactive neurons in the rat brain. Neuroscience 1985;16:917–48.

[90] Skofitsch G, Jacobowitz DM, Lembeck F. Galanin and vasopressin coexist in the rat hypothalamo–neurohypophyseal system. Neuroendocrinology 1989;49:419–27.

[91] Skofitsch G, Jacobowitz DM, Zamir N. Immunohistochemical localization of a melanin concentrating hormone-like peptide in the rat brain. Brain Res Bull 1985;15:635–49.

[92] Skofitsch G, Sills MA, Jacobowitz DM. Autoradiographic distribution of ^{125}I-galanin binding sites in the rat central nervous system. Peptides 1986;7:1029–42.

[93] Skofitsch G, Zamir N, Helke CJ, Savitt JM, Jacobowitz DM. Corticotropin releasing factor-like immunoreactivity in sensory ganglia and capsaicin sensitive neurons of the rat central nervous system: comparison with other neuropeptides. Peptides 1985;6:307–18.

[94] Steiner RA, Hohmann JG, Holmes A, Wrenn CC, Cadd G, Jureust A, et al. Galanin transgenic mice display cognitive and neurochemical deficits characteristic of Alzheimer's disease. Proc Natl Acad Sci USA 2001;98:4184–9.

[95] Strauss K, Jacobowitz DM, Schulkin J. Dietary calcium deficiency causes a reduction in calretinin mRNA in the substantia nigra compacta-ventral tegmental area of rat brain. Mol Brain Res 1994;25:140–2.

[96] Sutin EL, Jacobowitz DM. Immunocytochemical localization of peptides and other neurochemicals in the rat laterodorsal tegmental nucleus and adjacent area. J Comp Neurol 1988;270:243–70.

[97] Tatemoto K, Rökaeus A, Joernvall H, McDonald DI, Mutt V. Galanin—a novel biologically active peptide from porcine intestine. FEBS Lett 1983;164:124–8.

[98] Valentino KL, Eberwine IH, Barchas ID, editors. In situ hybridization. Applications to neurobiology. New York: Oxford University Press; 1987.

[99] Weiss JM, Bonsall RW, Demetrikopoulos MK, Emery MS, West CHK. Galanin: a significant role in depression. Ann NY Acad Sci 1998;863:364–82.

[100] Wrenn CC, Crawley JN. Pharmacological evidence supporting a role for galanin in cognition and affect. Prog Neuro-Psychoharmacol Biol Psychiat 2001;25:283–99.

[101] Wynick D, Small CJ, Bacon A, Holmes FE, Norman M, Ormandy CJ, et al. Galanin regulates prolactin release and lactotroph proliferation. Proc Natl Acad Sci USA 1998;95:12671–6.